Ultra-slow cratonic denudation in Finland since 1.5 Ga indicated by tiered unconformities and impact structures

Precambrian Research 352 (2021) 106000

Contents lists available at ScienceDirect

Precambrian Research

journal homepage: www.elsevier.com/locate/precamres

Ultra-slow cratonic denudation in Finland since 1.5 Ga indicated by tiered unconformities and impact structures

Adrian M. Hall [a,*], Niko Putkinen [b], Satu Hietala [c,d], Elina Lindsberg [d], Marko Holma [e,f,g]

[a] Department of Physical Geography, Stockholm University, S-10691 Stockholm, Sweden
[b] Geological Survey of Finland, P.O. Box 97, FI-67101 Kokkola, Finland
[c] Department of Geology, University of Tartu, Ravila 14A, 50411 Tartu, Estonia
[d] Geological Survey of Finland, P.O. Box 1237, FI-70211 Kuopio, Finland
[e] Muon Solutions Oy, Rakkarinne 9, FI-96900 Saarenkylä, Finland
[f] Kerttu Saalasti Institute, University of Oulu, Pajatie 5, 85500 Nivala, Finland
[g] Arctic Planetary Science Institute, Lihtaajantie 1 E 27, 44150 Äänekoski, Finland

ARTICLE INFO

Keywords:
Craton
Unconformity
Impact structure
Denudation
Thermochronology
Finland

ABSTRACT

The Earth's cratons are traditionally regarded as tectonically stable cores that were episodically buried by thin sedimentary covers. Cratonic crust in southern Finland holds seven post-1.7 Ga tiered unconformities, with remnants of former sedimentary covers. We use the geometries of the tiered unconformities, along with previously dated impact structures and kimberlite and carbonatite pipes, to reconstruct the erosion and burial history of the craton and to derive estimates of depths of erosion in basement and former sedimentary rocks. The close vertical spacing (<200 m) of the unconformities and the survival of small (D ≤ 5 km) Neoproterozoic and Early Palaeozoic impact structures indicate minor later erosion. Average erosion rates (<2.5 m/Ma) in basement and cover are amongst the lowest reported on Earth. Ultra-slow erosion has allowed the persistence in basement fractures of Phanerozoic fracture coatings and Palaeogene groundwater and microbiomes. Maximum thicknesses of foreland basin sediments in Finland during the Sveconorwegian and Caledonide orogenies are estimated as ~1.0 km and <0.68–1.0 km, respectively. Estimated losses of sedimentary cover derived from apatite fission track thermochronology are higher by factors of at least 2 to 4. A dynamic epeirogenic history of the craton in Finland, with kilometre-scale burial and exhumation, proposed in recent thermochronological models is not supported by other geological proxies. Ultra-slow erosion rates in southern Finland reflect long term tectonic stability and burial of the craton surface for a total of ~1.0 Ga beneath generally thin sedimentary cover.

1. Introduction

Cratons hold the Earth's oldest rocks and landscapes. Yet cratonic denudation rates are poorly known over geological timescales because even slow denudation, if sustained, eventually removes evidence of its surface operation. Sedimentary and volcanic rocks and weathering mantles that constrain the depth and timing of erosion and burial on platforms (Gunnell, 2020) are generally missing from shields, including regions eroded by Late Cenozoic ice-sheets (André et al., 2001). In the absence of such proxies, thermochronometry has become the standard tool for reconstructing thermal histories (Kohn and Gleadow, 2019). Yet current thermochronological models often struggle to replicate cratonic denudation acting slowly at the sub-kilometre scale (Gunnell, 2000; Vasconcelos and Carmo, 2018). There is a pressing need to test thermochronological models for cratons against independent geological evidence (Green et al., 2020).

In this paper, we examine the erosion and burial history of the craton in southern Finland. Finland is exceptional as it retains inherited basement landforms, traces of sedimentary cover rocks, volcaniclastic kimberlite dykes and many eroded impact structures (IMPs) (Fig. 1A). These features indicate that the craton has experienced multiple megacycles of uplift, erosion, relief reduction and burial since 1.7 Ga. We derive high-resolution estimates of depths and rates of erosion in basement and cover rocks from basement unconformities and the geometries of previously dated IMPs. The revealed erosion rates are amongst the lowest reported on Earth and indicate exceptional stability and prolonged, shallow burial of the craton. Existing thermochronological models significantly overestimate the thicknesses of former sedimentary

* Corresponding author.
E-mail address: adrian.hall@natgeo.su.se (A.M. Hall).

https://doi.org/10.1016/j.precamres.2020.106000
Received 24 August 2020; Received in revised form 29 October 2020; Accepted 2 November 2020
Available online 6 November 2020

cover in Finland.

2. Geological setting

The Precambrian continental crust was assembled in southern Finland towards the close of the Svecofennian orogeny at 1.76 Ga (Nironen, 2017). Final stabilisation of the crust followed intrusion of rapakivi granites and dyke swarms at 1.65–1.47 Ga (Korja et al., 2006). Following uplift and unroofing of rapakivi granites, basement surfaces were buried at 1.5–1.4 Ga (Lundmark and Lamminen, 2016) beneath thick Mesoproterozoic ("Jotnian") arkosic sandstones now preserved in extensional intra-cratonic basins around the present Bothnian Sea and Lake Ladoga (Fig. 1A, B). Mesoproterozoic sedimentary cover rocks were intruded by dykes and sills at 1.27–1.1 Ga (Buntin et al., 2019) at the onset of the Sveconorwegian orogeny (Slagstad et al., 2020) (Fig. 2). The approximate extent of the former foreland basin of the orogen is delineated by the ~200 km-wide Blekinge-Dalarna dyke swarm in southern and central Sweden (Ripa and Stephens, 2020) (Fig. 1A). Foreland basin sedimentation may have extended towards Finland (Larson et al., 1999), but the extent and thickness of former platform sediments is uncertain (Kohonen and Rämö, 2005).

Early- and Mid-Neoproterozoic (Tonian-Cryogenian, 1000–640 Ma) sedimentary rocks are missing in onshore Finland. This hiatus likely marks a long period of erosion after 900 Ma when Jotnian and younger cover rocks were removed from the shield surface outside intracratonic basins (Puura et al., 1996). Denudation culminated with levelling of basement across Baltica by the Late Neoproterozoic (Kohonen and Rämö, 2005). From the Late Ediacaran (~550 Ma) onwards, marine transgression across Baltica led to burial by Early Palaeozoic sandstones, shales and limestones (Nielsen and Schovsbo, 2011) that reach a total thickness of 400 m in Estonia (Kirsimäe et al., 1999). During the Caledonian orogeny (~420–350 Ma), thermochronology suggests further burial to depths of 3–4 km in foreland basins in eastern Sweden (Tullborg et al., 1995), perhaps reaching 6 km (Huigen and Andriessen, 2004; Samuelsson and Middleton, 1998), but the context, extent and thickness of Silurian to Permian cover in Fennoscandia are disputed (Hendriks and Redfield, 2005). East of Lake Onega, Palaeozoic cover is restricted to Late Devonian sandstones and shales; these rocks and underlying Late Ediacaran sediments and basement were exposed to weathering in the Early Carboniferous, with formation of bauxites (Mordberg and Nesterova, 1996). Palaeozoic cover on the southern edge of the platform was thinned by erosion in the Early Permian (300 Ma) in response to a phase of magmatism and uplift, recorded by dyke swarms, fault reactivation and low-temperature hydrothermal alteration (Preeden et al.,

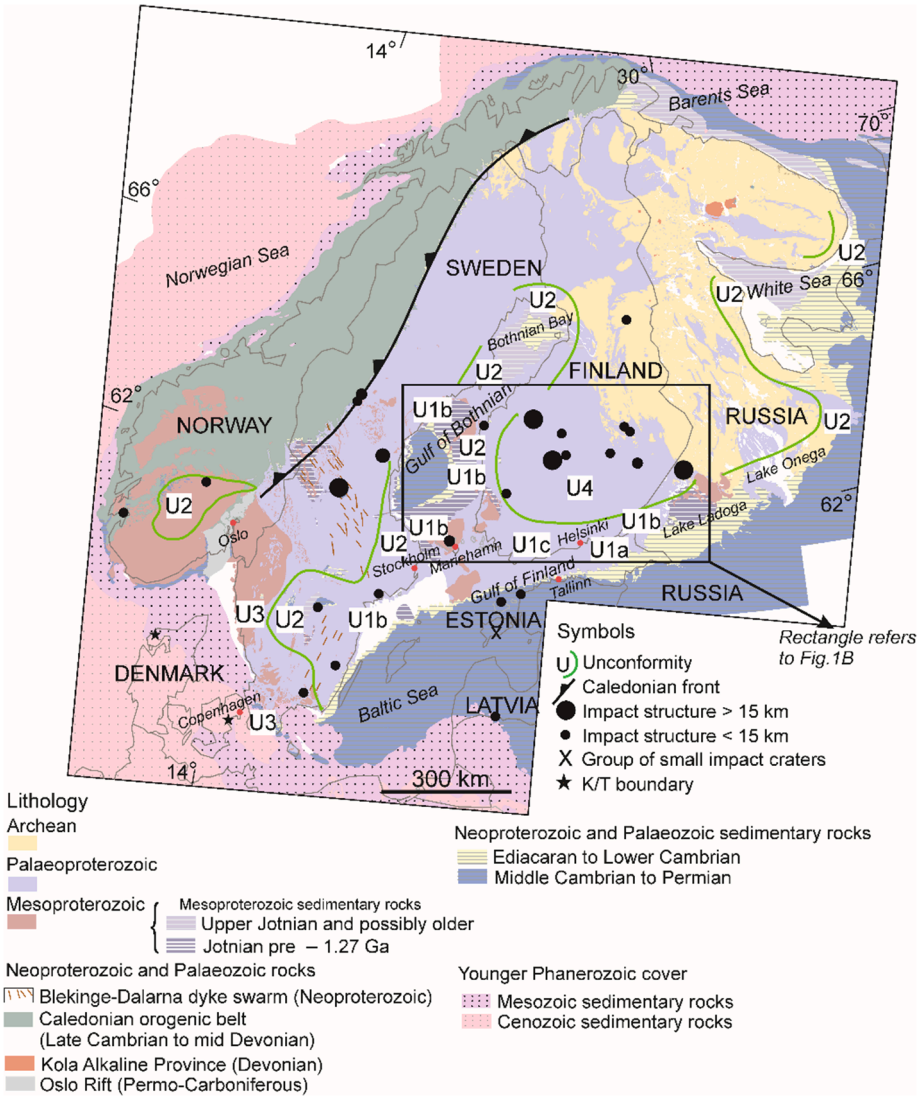

Fig. 1. Geology of the craton in southern finland and its surroundings simplified geology of fennoscandia showing main rock groups, locations of the main basement unconformities and impact structures. modified after (Koistinen et al., 2001). Geology of the craton in southern Finland and its surroundings. The topographic profile lines refer to Fig. 3.

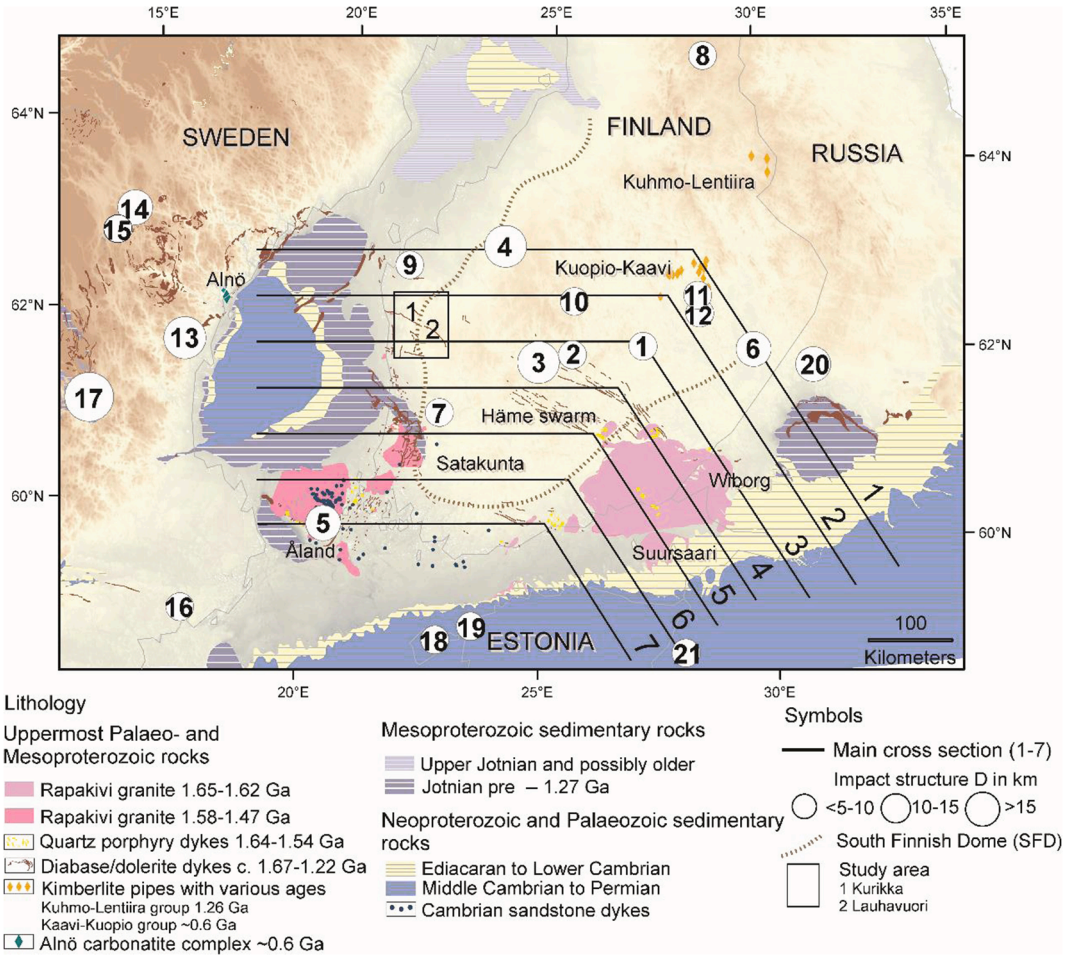

Fig. 1. (*continued*).

2009) associated with the break-up of Pangaea (Holm et al., 2010). Across southernmost Sweden, progressive re-exposure of the shield surface is demonstrated by weathered basement unconformities of Late Triassic and Late Cretaceous age (Japsen et al., 2016; Lidmar-Bergström et al., 1997). Finland mainly remained above sea level through the Mesozoic (Torsvik and Cocks, 2016); no Mesozoic sedimentary rocks are recorded from the Late Cretaceous IMPs. Through the Palaeogene and Neogene, the Bothnian and Gulf of Finland depressions formed routeways for the vast Eridanos or Baltic River drainage system that transported sediment southward (Gibbard and Lewin, 2016). Kilometre-scale uplift along the North Atlantic margin in the Neogene (Stuevold and Eldholm, 1996) was associated with tilting of the backslope across eastern Sweden and uplift of epeirogenic domes in Fennoscandia, including the South Finnish Dome (SFD) (Fig. 1B). Increased sediment volumes in the eastern North Sea Basin indicate significant acceleration of erosion across Fennoscandia from the early Miocene (Rasmussen, 2018). In Finland, the land surface was lowered during multiple phases of deep weathering and stripping (Söderman, 1985; Tanner, 1938). The Fennoscandian Ice Sheet (FIS) developed after 2.7 Ma but remained largely restricted in its extent until ~1.2 Ma. Subsequent glacial erosion removed Early Palaeozoic sedimentary cover from the Bothnian and Baltic basins and their surroundings (Amantov, 1995; Hall and van Boeckel, 2020). Depths of erosion were low (<20 m) in basement areas where the sub-Cambrian unconformity was re-exposed by erosion beneath the FIS (Hall et al., 2019a, 2019b).

3. Estimation of Proterozoic and Phanerozoic erosion in southern Finland from geological proxies

3.1. Unconformities

Multiple basement unconformities are identified in Finland which mark the terminations of erosion phases at intervals in the Proterozoic (U1), Early Palaeozoic (U2); Mesozoic (U3), Cenozoic (U4) and Quaternary (UQ) (Figs. 1A and 2). The unconformities are closely spaced laterally and vertically (Figs. 1 and 3) and are referred to as *tiered unconformities*. Separate unconformities are recognised at 1.7–1.6 Ga (U1a), 1.5 Ga (U1b) and 0.9 Ga (U1c) within the Proterozoic Eon in Finland. U2 extended across much of Baltica by the end of the Ediacaran (Nielsen and Schovsbo, 2011). This palaeo-surface has been widely referred to in Scandinavia as the *Sub-Cambrian Peneplain* in recognition of its smooth, near-planar form where it emerges from beneath Early Palaeozoic cover rocks (Lidmar-Bergström, 1993). In southern Sweden, younger weathered basement unconformities are buried by Late Triassic (U3a) and Late Cretaceous (U3b) sedimentary cover (Japsen et al., 2016). Exposed basement in Finland was deeply weathered under warm and humid environments in the Palaeogene and Neogene (Gilg et al., 2013; Hall et al., 2015), a phase in which an epigene palaeo-surface (U4) was cut across the crest of the SFD. UQ is locally buried by mainly thin Late Quaternary glacial sediments.

The relative ages of unconformities are apparent from cross-cutting relationships. Younger epigene surfaces cut exhumed unconformities and carry weathering covers that provide age estimates for the timing of young episodes of planation. The minimum ages of exhumed unconformities are provided by sedimentary covers, including outliers

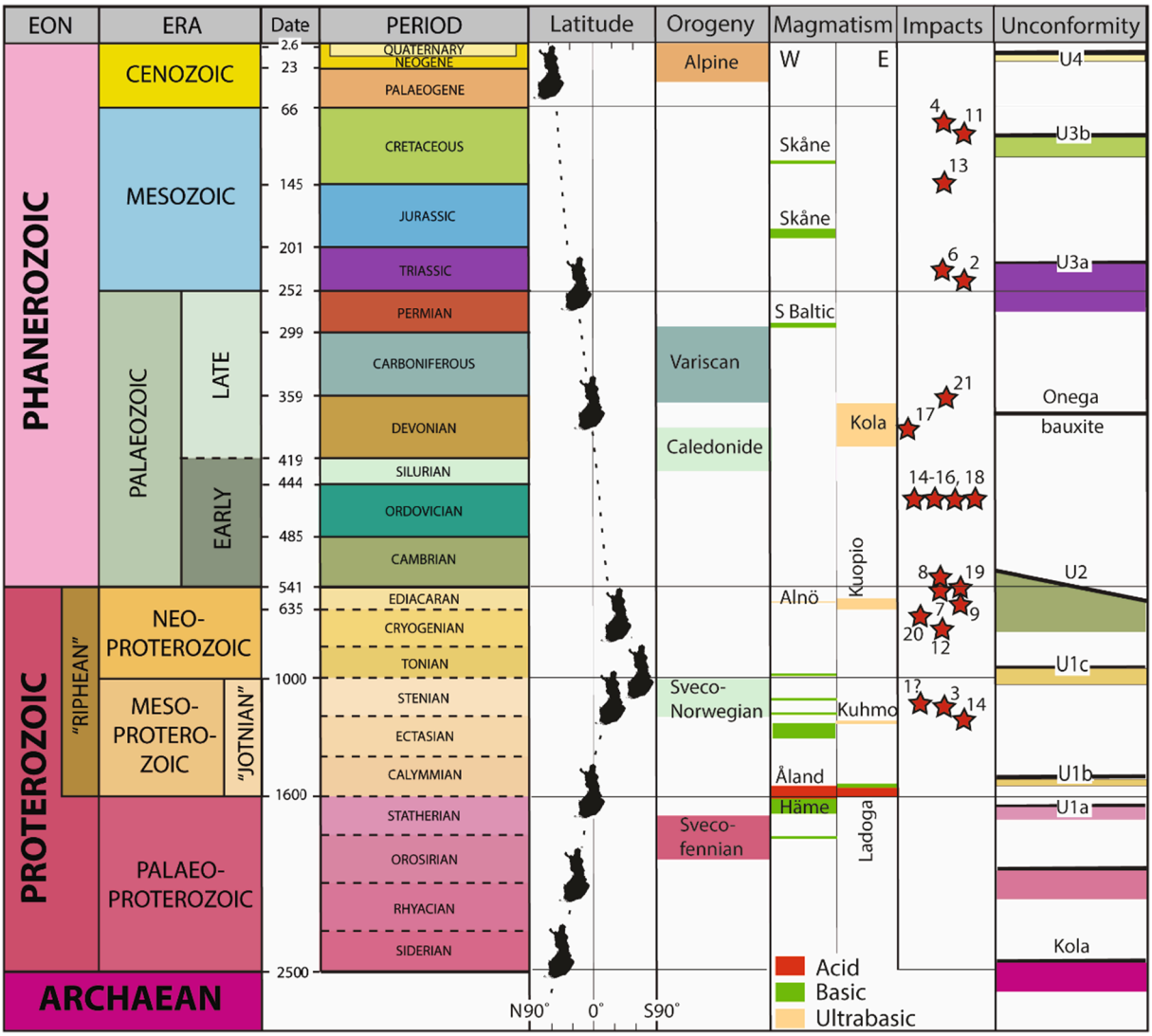

Fig. 2. Main events in the history of the craton. Geological timescale from Gradstein et al. (2012). Position of the craton on Earth through time from Tikkanen (2002). Timings of magmatism on the craton are referred to in the text. IMP details in Table 1. The main basement unconformities are shown as lines and represent the culminations of periods of erosion which are shown by shading.

preserved in IMPs (Puura and Plado, 2005). The 2-D form of the palaeosurfaces is reconstructed in profiles projected from beneath sedimentary cover (Fig. 3). Negative relief on U1b is reconstructed in Ostrobothnia where remnants of Mesoproterozoic sandstone have been discovered in drilling and seismic surveys on basement valley floors (Fig. 4.). The elevation differences between basement unconformities of known ages represent the depths of basement rock removed in the intervals between the formation of the unconformities.

3.2. Impact structures

Southern Finland and its environs hold a remarkable array of IMPs (Fig. 1B), amongst the densest concentrations on Earth (Abels et al., 2002). Notably, many IMPs are not only small ($D \leq 5$ km), but old, with mainly Neoproterozoic and Early Palaeozoic ages (Table 1). The ages of IMPs in Finland are generally well constrained by sedimentary fills and radiometric ages (Table 1), notwithstanding the challenges of dating impact rocks (Jourdan et al., 2012; Schmieder and Kring, 2020). All IMPs considered here, except Keurusselkä, retain impact breccias and, in many cases, the depth of the base of impact breccias below the present land surface, d_p, has been identified through drilling or geophysical surveys (Table 1). Impact targets were exposed shield surfaces or thin platform cover; impacts occurred in terrestrial or marine settings (Puura and Plado, 2005) (Table 1).

IMPs provide important evidence of post-impact erosion histories (Masaitis, 2005; Puura and Plado, 2005). An empirical relationship has been established previously between the original diameter (D) and original depth (d_t) of IMPs from 31 morphologically well-preserved, simple and complex, terrestrial impact craters on Earth (Degeai and Peulvast, 2006). Original depth is the datum represented by the base of impact breccias (Fig. 5). The total post-impact erosion depth since impact, e_d, is derived by subtraction of d_p from d_t. Where d_p is unknown, the maximum depth of rock lost to erosion is constrained only by d_t. Significant uncertainties (>30%) exist in estimating d_t in the Earth dataset due to differences between terrestrial and marine target settings, in rock substrates and in impact trajectories (Degeai and Peulvast, 2006). Maximum ($0.184\ D^{0.54}$), mid-range ($0.133\ D^{0.57}$) and minimum ($0.095\ D^{0.60}$) values for d_t are estimated for IMPs in Finland and neighbouring areas (Table 2), with the mean value of d_t cited below (Table 2).

IMPs at Söderfjärden and Kärdla have been buried since impact and preserve original crater forms (Puura and Plado, 2005). In both cases, d_p is known and must approximate to d_t. Application of the empirical relationship of Degeai and Peulvast (2006) at Söderfjärden ($D = 6.6$ km)

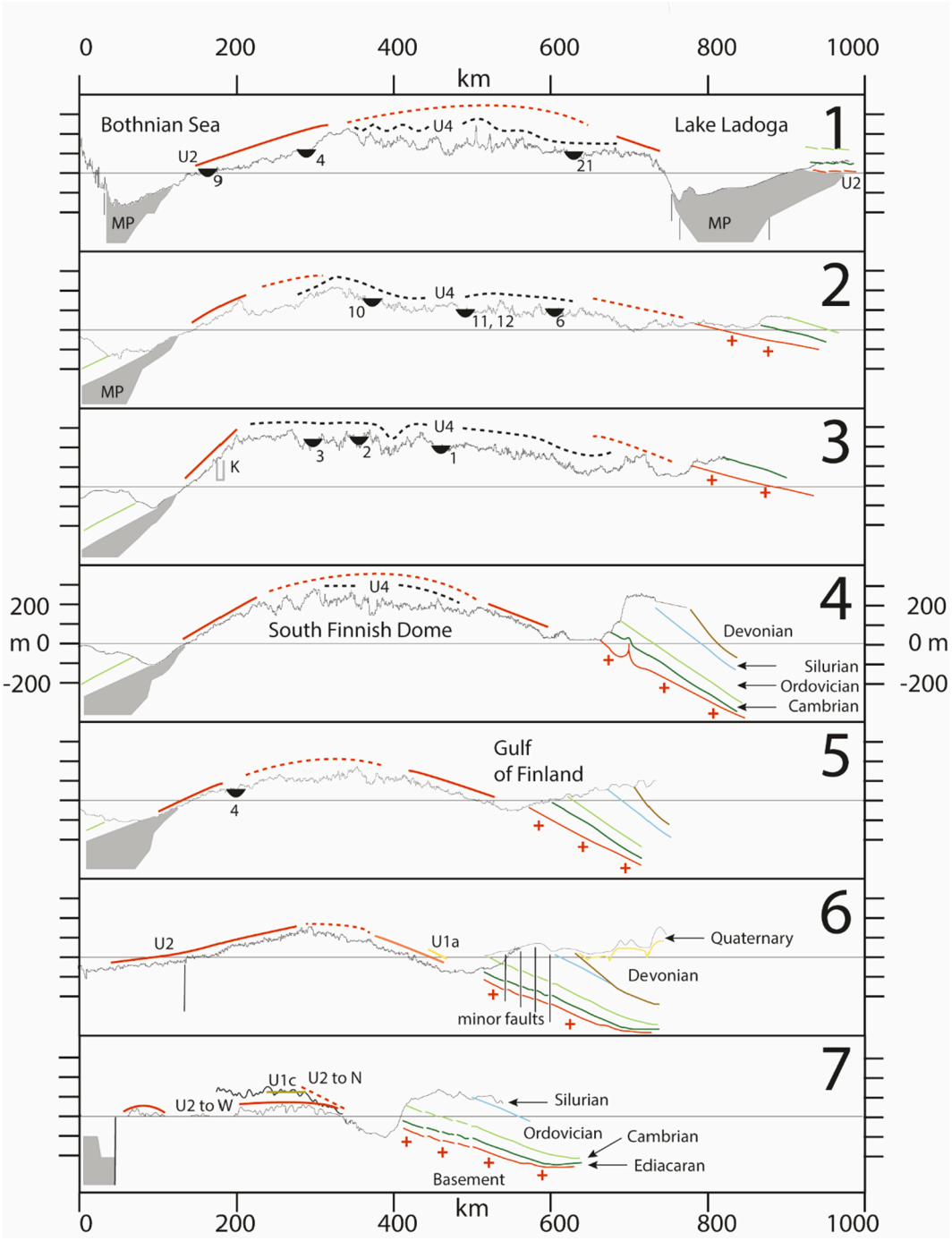

Fig. 3. The craton surface and its sedimentary cover in southern Finland The positions of unconformities, impact structures and cover rocks are shown. Topographic profiles 1–7 are indicated on Fig. 1B.

provides an estimate for d_t of 390 m that compares to a drilled depth of 320 m (Lehtovaara, 1982; Öhman and Preeden, 2013). At Kärdla (D = 4 km), the estimated d_t is 290 m and the drilled depth of impact breccias below fall-back breccias on the crater flow is 220 m (Suuroja et al., 2002). These two examples provide support for the application of the empirical relationship to the study area. We note also that the survival of small IMPs (D≤5 km) permits only limited depths of erosion ($d_t \leq 300$ m).

Where IMPs hold remnants of former cover rocks or are located proximal to sedimentary cover, the depths of basement and cover eroded can be estimated and average rates of post-impact erosion can be derived (Table 2).

3.3. Other geological proxies

Various well-dated geological indicators of burial and erosion depths exist in southern Finland and its immediate surroundings (Fig. 1B). The diagenetic characteristics of sedimentary rocks provide broad indications of former burial temperatures and depths (Kirsimäe et al., 1999). The layer-cake stratigraphy of the Palaeozoic cover south of the Gulf of Finland (Fig. 3) allows the approximate thickness of missing sedimentary section to be estimated for southern Finland. Comparisons with model forms of vertically-zoned, sub-volcanic igneous dykes (Gudmundsson, 1983), carbonatite pipes (Fontana, 2006) and volcaniclastic kimberlite pipes (Hawthorne, 1975) provide broad estimates of

Table 1
Impact structures in Finland and the surroundings.

	Name	Coordinates		Diameter [kilometres]	Age [Ma]*This paper*	Target setting	Target rocks	Simple/ Complex	IMP fill	Reference(s)
	Finland	Northing	Easting							
1	Iso-Naakkima[1]	62°11′	27°09′	3	*~550*	T	B	S	MP, NP[1]	(Elo et al., 1993; Järvelä et al., 1995; Pesonen et al., 1996; Schmieder and Kring, 2020)
2	Karikkoselkä[2]	62°15′	25°15′	1.5	~260–230, 9[2]	T	B, NP, C, O	S		(Pesonen et al., 1999; Uutela, 2001)
3	Keurusselkä	62°08′	24°36′	14–36	1151 ± 10	T	B	C		(Osinski and Ferrière, 2016; Raiskila et al., 2011; Schmieder et al., 2009, 2016; Hietala and Moilanen, 2007)
4	Lappajärvi	63°12′	23°42′	23	78.9 ± 0.78	T	B, C, O	C		(Kenny et al., 2019; Schmieder and Jourdan, 2013)
5	Lumparn	60°09′	20° 08′	10	≤458	M	O	C	D	(Abels et al., 1998; Merrill, 1980)
6	Paasselkä	62°08′	29°23′	10	231 ± 2.2	T	B, NP	C?		(Abels et al., 2002; Schmieder et al., 2008, 2010; Schwarz et al., 2015)
7	Sääksjärvi	61°25′	22°23′	6	608 ± 8	T	B, MP	S?		(Abels et al., 2002; Kenny et al., 2020)
8	Saarijärvi	65°17′	28°23′	2.2	<600–520	M	B, NP, C	S		(Öhman, 2002, 2007)
9	Söderfjärden	62°41′	21°35′	6.6	~640 *~540–520*	T	B, C	C	O, D	(Abels, 2003; Abels et al., 2002; Schmieder et al., 2014)
10	Summanen	62°39′	25°23′	3	<1880	T	B	S		(Plado et al., 2018; Hietala and Moilanen, 2007; Hietala et al., 2020)
11	Suvasvesi, North	62°41′	28°11′	3.5	~85	T	B	C		(Abels et al., 2002; Schmieder et al., 2016)
12	Suvasvesi, South	62°41′	28°11′	3.8	~710	T	B	S		(Schmieder et al., 2016a)
	Sweden									
13	Dellen	61°50′	16°45′	19	140.8 ± 0.51	T	B	C		(Mark et al., 2014)
14	Lockne	63°0′	14°49′	7.5–14	455 ± 1	M	O	C		(Lindström et al., 1996; Schmieder and Kring, 2020; Sturkell and Lindström, 2004)
15	Målingen	62°55′	14°33′	0.7	455 ± 1	M	O	S		(Örmö et al., 2014)
16	Tvären Bay	58°46′	17°25′	2	~458	M	O	S		(Ormö, 1994)
17	Siljan	61°02′	14°52′	52–90	380.9 ± 4.6	T		C		(Holm et al., 2011; Jourdan et al., 2012)
	Estonia									
18	Kärdla	59°1′	22°46′	4	455 ± 1	M	O	C	O	(Jõeleht et al., 2018; Plado, 2012; Grahn et al., 1996)
19	Neugrund	59°20′	23°40′	6–20	~540–530	M	C	C	O	(Suuroja and Suuroja, 2004, 2010)
	Russia									
20	Jänisjärvi	61°58′	30°58′	14	687 ± 5	T	NP	C		(Jourdan et al., 2008)
21	Mishina Gora	58°43′	28°3′	2.5	<360	T	D	S		(Masaitis, 1999)

Target settings are marine (M) or terrestrial (T). Target rocks are basement (B) or cover rocks of Mesoproterozoic (MP), Neoproterozoic (NP), Cambrian (C), Ordovician (O) or Devonian (D) ages. IMP fills are abbreviated similarly. IMP structures are simple (S) or complex (C) (Fig. 5).
[1] See text for discussion of target geology [2]Also anomalous 9 Ma age (Schmieder et al. 2010) [3]See text for discussion of IMP age [4]IMP lacks drill data

post-cooling erosion depths.

We compare the erosion and burial history reconstructed from the tiered unconformities, IMPs and other erosion depth indicators with published cooling ages derived from low-temperature thermochronology across southern Finland (Fig. 6).

4. Erosion and burial history of the craton in Finland

The oldest unconformities in Fennoscandia are found on Late Archaean granitoid basement and within metamorphosed supracrustal sequences (Kirsimäe and Melezhik, 2013). These include a weathered unconformity dating from 2.45 to 2.33 Ga that extends across northern Norway and Finland and into Kola at the base of the 10 km thick Petsamo Supergroup (Soomer et al., 2019; Sturt et al., 1994). Another weathered unconformity is found in Karelia, with a younger origin from 2.3 Ga (Strand, 2012). A Paleoproterozoic lateritic palaeosol is overlain by mature quartzite and dated to 1.87–1.84 Ga in south-west Finland (Lahtinen and Nironen, 2010). This unconformity occurs within the Svecofennian orogen and predates regional stabilisation of the crust.

4.1. Palaeoproterozoic and Mesoproterozoic

The onset of crustal stabilisation in southern Finland is marked by U1a, developed between 1.76 and 1.65 Ga (Pokki et al., 2013b). At Suursaari (Pokki et al., 2013b) and east of the Wiborg rapakivi granite (Puura and Flodén, 1999) (Fig. 1B), hilly basement surfaces are overlain by unmetamorphosed quartz conglomerates. U1a in SE Finland stands at almost the same erosional level as U2, formed by 550 Ma, and the present basement surface (Pokki et al., 2013b). Mature, quartz-rich sedimentary rocks also occur in a 10 km wide roof pendant on the Wiborg rapakivi batholith (Pokki et al., 2013b) and as small, foundered blocks in the 1.64 Ga Häme dolerite dyke swarm (Laitakari and Leino, 1989). Undevitrified volcanic glass and amygdales are found in this dyke swarm (Lindqvist and Laitakari, 1980) and in contemporaneous swarms at Satakunta (Mertanen, 2008) and Åland (Salminen et al., 2017). Comparisons with Plio-Pleistocene dykes beneath lava flows in Iceland (Gudmundsson, 1983) suggest that degassing of the Häme dykes took place at depths of 0.5–1 km. Hence, the present basement surface in SW Finland stands within 1 km of U1a (Fig. 3: profiles 6 & 7). Post-U1a quartz conglomerates are unknown further N in Finland, indicating non-deposition or removal by erosion.

An extensive, younger basement unconformity, U1b (Fig. 1A), emerges from beneath Mesoproterozoic ("Jotnian") sedimentary cover around the Bothnian basin and is referred to as the "sub-Jotnian unconformity" in older literature (Högbom, 1910; von Eckermann, 1937). In eastern Sweden, U1b shows areas of low relief and hilly terrain (Hall

Table 2
Erosion depth calculations for impact structures.

	Name	Apparentdiameter(km)	Maximumoraccurateage(Ma)	Presentelevationa.s.l.aroundimpactstructure	Preservationlevel*	Rim − to − rimdiameter(km)(D)	Originaldepthmaximum(km)(d_t)	Originaldepthmid − range(km)(d_t)	Originaldepthminimum(km)(d_t)	Brecciabasedepthfrompresentsurface	Brecciabaseelevationbelowpresent(d_p)	Maximumrelativepalaeoelevationatimpact	Mid − rangepalaeoelevationatimpact	Minimumpalaeoelevationatimpact	Thicknessofrocklostmaximum	Thicknessofrocklostmid − range	Thicknessofrocklostminimum	Longtermmaxrateoferosion(m/Myr)	Longtermmid − rangerateoferosion(m/Myr)imum	Longtermaverageminimumrateoferosion(m/Myr)
Finland																				
1	Iso-Naakkima	2.5	550	0.12	6	3	0.33	0.25	0.18	0.15	−0.03	0.30	0.22	0.15	0.18	0.10	0.03	0.33	0.18	0.06
2	Karikkoselkä	1.5	260–230	0.13	5	1.5	0.23	0.17	0.12	0.12	0.01	0.24	0.18	0.13	0.11	0.05	0.00	0.42–0.47	0.18–0.20	0.00–0.01
3	Keurusselkä	14	1151	0.14	7	36	1.27–0.77	1.03–0.60	0.82–0.46	−0.2	0.34	1.61–1.11	1.37–0.94	1.16–0.80	1.47–0.97	1.23–0.80	1.02–0.66	1.28–0.84	1.06–0.69	0.88–0.58
4	Lappajärvi	23	78	0.12	5	23	1.00	0.79	0.62	0.6	−0.48	0.52	0.31	0.14	0.40	0.19	0.02	5.13	2.49	0.30
5	Lumparn	10	≤458	0.05	5	10	0.64	0.49	0.38	0.09	−0.04	0.60	0.45	0.34	0.55	0.40	0.29	1.20	0.88	0.63
6	Paasselkä	10	231	0.11	6	10	0.64	0.49	0.38	0.25	−0.14	0.50	0.35	0.24	0.39	0.24	0.13	1.68	1.06	0.55
7	Sääksjärvi	6	608	0.07	5	6.0	0.48	0.37	0.28	0.11	−0.04	0.45	0.33	0.24	0.38	0.26	0.17	0.62	0.43	0.29
8	Saarijärvi	1.5	600–520	0.27	5	2.2	0.28	0.21	0.15	0.16	0.11	0.39	0.32	0.26	0.12	0.05	−0.01	0.20–0.13	0.08–0.01	−0.01– −0.07
9	Söderfjärden	6.6	540	0.03	5	6.6	0.51	0.39	0.29	0.35	−0.32	0.19	0.07	−0.03	0.16	0.04	−0.06	0.30	0.07	−0.10
10	Summanen	3	<1880	0.15	5	3	0.33	0.25	0.18											
11	Suvasvesi. North	3.5	85	0.13	5	3.5	0.36	0.27	0.20	0.26	−0.13	0.23	0.14	0.07	0.10	0.01	−0.06	1.20	0.14	−0.69
12	Suvasvesi. South	3.8	710	0.13	5	3.8	0.38	0.28	0.21	0.26	−0.13	0.25	0.15	0.08	0.12	0.02	−0.05	0.17	0.03	−0.07
Sweden																				
13	Dellen	19	141	0.3	4	19	0.90	0.71	0.56	0.75	−0.45	0.45	0.26	0.11	0.15	−0.04	−0.19	1.08	−0.27	−1.38
14	Lockne	7.5	455	0.43	2	7.5	0.55	0.42	0.32							0.00				
15	Målingen	0.7	455	0.36	3	1	0.18	0.13	0.10	0.08	0.28	0.46	0.41	0.38	0.10	0.05	0.02	0.23	0.12	0.03
16	Tvären Bay	2	458	0	5	2	0.27	0.20	0.14	0.14	−0.14	0.13	0.06	0.00	0.13	0.06	0.00	0.28	0.13	
17	Siljan	52	380	0.35	7	90–52	2.09–1.55	1.73–1.26	1.41–1.02	0.6	−0.25	1.84–1.30	1.48–1.01	1.16–0.77	1.49–0.95	1.13–0.66	0.81–0.41	3.92–2.51	2.97–1.75	2.14–1.10
Estonia																				
18	Kärdla	4	455	−0.05	2	4	0.29									0				
19	Neugrund	6	~540–530	−0.05	2	20	0.73									0				
Russia																				
20	Jänisjärvi	14	687	0.1	5	14	0.65													
21	Mishina Gora	2.5	<360	0.07	5	2.5	0.22	0.22	0.16	0.6	−0.53	−0.31	−0.31	−0.37	−0.38	−0.38	−0.44	−1.04	−1.04	−1.21

Preservation level after Puura and Plado (2005). 1. Ejecta largely preserved. 2. Ejecta partly preserved. 3. Ejecta removed, rim partly preserved. 4. Rim largely eroded, crater-fill preserved. 5. Crater-fill products partly preserved. 6. Remnants of crater-fill preserved, crater floor exposed. 7. Crater floor exposed, substructure exposed.

et al., 2019a).

In western Finland, drilling, aeromagnetic and resistivity surveys for groundwater research have revealed a 100 m deep valley system cut in Palaeoproterozoic gneisses (Fig. 4), with thick fills of Pleistocene sediment (Pitkäranta, 2013). At Karhukangas (Fig. 4C), the valley floor retains >10 m of sandstone (Huhta, 1997) of similar lithology to Mesoproterozoic sandstones in the Bothnian Sea and the Satakunta half-graben (Pokki et al., 2013a). We interpret the valley system as part of hilly topography on U1b formed during or after 1.55 Ga magmatism, filled by sands by 1.27 Ga and re-excavated during the Late Cenozoic. The palaeo-valley floors stand up to 200 m below the base of the Early Cambrian sandstone outlier at Lauhanvuori. Basal Cambrian conglomerates include pebbles of red arkosic sandstone (Söderman et al., 1983), indicating the presence of eroding Mesoproterozoic sandstones nearby during sedimentation. Localised concentrations of glacial erratics suggest that other small outliers of Mesoproterozoic sandstone may exist in south-central Finland (Donner, 1996; Paulamäki and Kuivamäki, 2006).

U1b is younger in age around Lake Ladoga, cut across rapakivi granites dated to 1547–1530 Ma and overlain by sedimentary and volcanic rocks dated to 1499 Ma (Velichkin et al., 2005). Here U1b dips gently to the south-west (Rice-Bredin, 2012). Roof pendants on the Wiborg rapakivi granite indicate ~3 km of missing volcanic superstructure (Vorma, 1975). Fault block mountains were present on the rapakivi granites (Puura and Plado, 2005). Basement areas between rapakivi intrusions across southern Finland remained close to the erosion level of U1a (Koistinen, 1996), indicating that large differential movements across shear zones occurred during granite emplacement (Mertanen et al., 2008).

Erosion of the Jotnian cover on U1b and lowering of its irregular basement surface occurred at 1.42 Ga in eastern Sweden (Drake et al., 2009). The large Keurusselkä IMP (Fig. 1B) in south-central Finland has a $^{40}Ar/^{39}Ar$ date of 1150 ± 10 Ma (Schmieder et al., 2016a), one of the oldest ages for an IMP on Earth. Original diameters of 14 km and up to 25–36 km have been proposed (Hietala and Moilanen, 2007; Osinski and Ferrière, 2016; Raiskila et al., 2011). Today, it is eroded down close to the base of its former impact breccia layer (Raiskila et al., 2013), indicating a post-impact erosion depth of 0.80–1.23 km (Table 2). Kimberlite dykes emplaced at 1.21–1.18 Ga in the Kuhmo-Lentiira area (Dalton et al., 2020) (Fig. 1B) represent the deeply (>1.0 km) eroded roots of former kimberlite diatremes (O'Brien, 2015). The preservation of U1a ~200 km to the south and U1b ~100 km to the west, indicates that this 1 km depth erosion did not occur in the basement. Instead, erosion involved the removal of Mesoproterozoic sedimentary cover, a loss of overburden that is consistent with estimates for Proterozoic cover rock thicknesses of up to 0.5–2.0 km (Puura et al., 1996). The absence from Finland of small Mesoproterozoic IMPs likely reflects protection of basement beneath sedimentary cover.

The IMP at Iso-Naakkima, 130 km E of Keurusselkä, has a palaeomagnetic age of 1200–900 Ma (Pesonen et al., 1996). Survival of this small crater (D = 2.5 km), however, requires <220 m of erosion and so

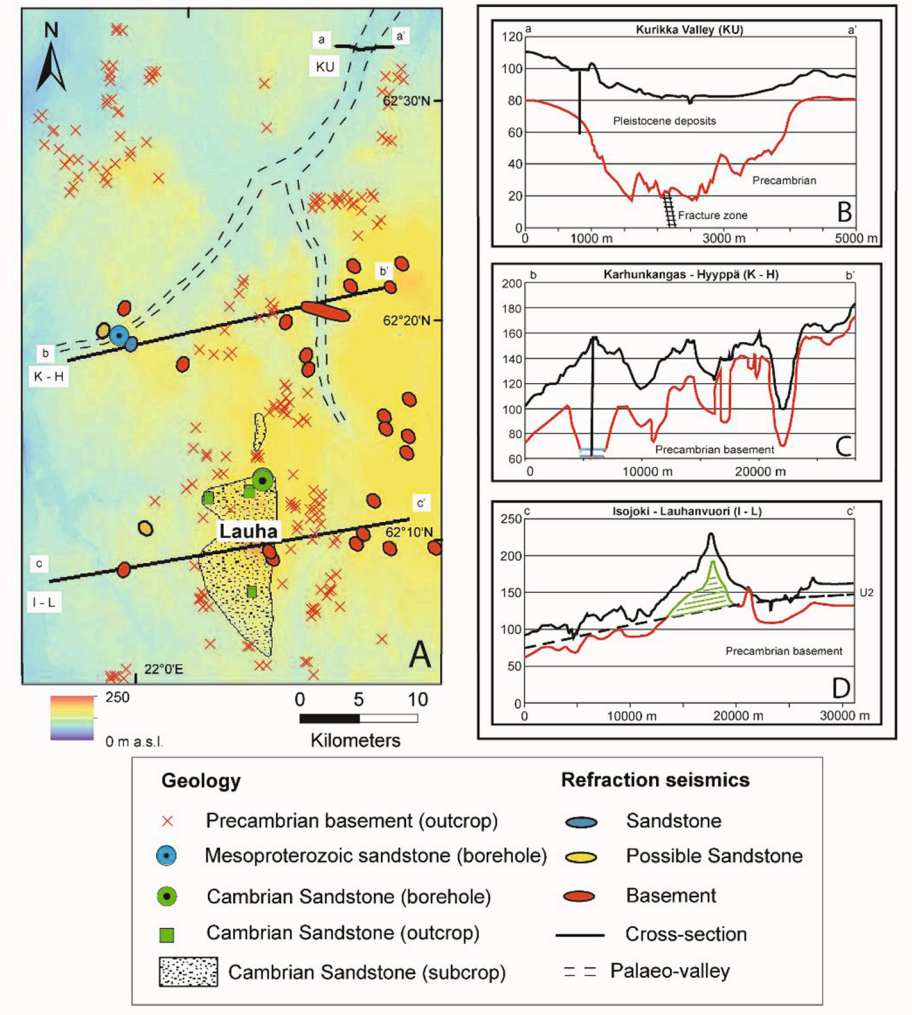

Fig. 4. Palaeo-topography on U1b and U2 in Ostrobothnia. A. Palaeo-valley systems on U1b with Mesoproterozoic sandstone at Kurikka and the outlier of Early Cambrian sandstone on U2 at Lauhanvuori. Cross-sections B-D showing the basement valleys, the sedimentary rock outliers and the Pleistocene sediment cover.

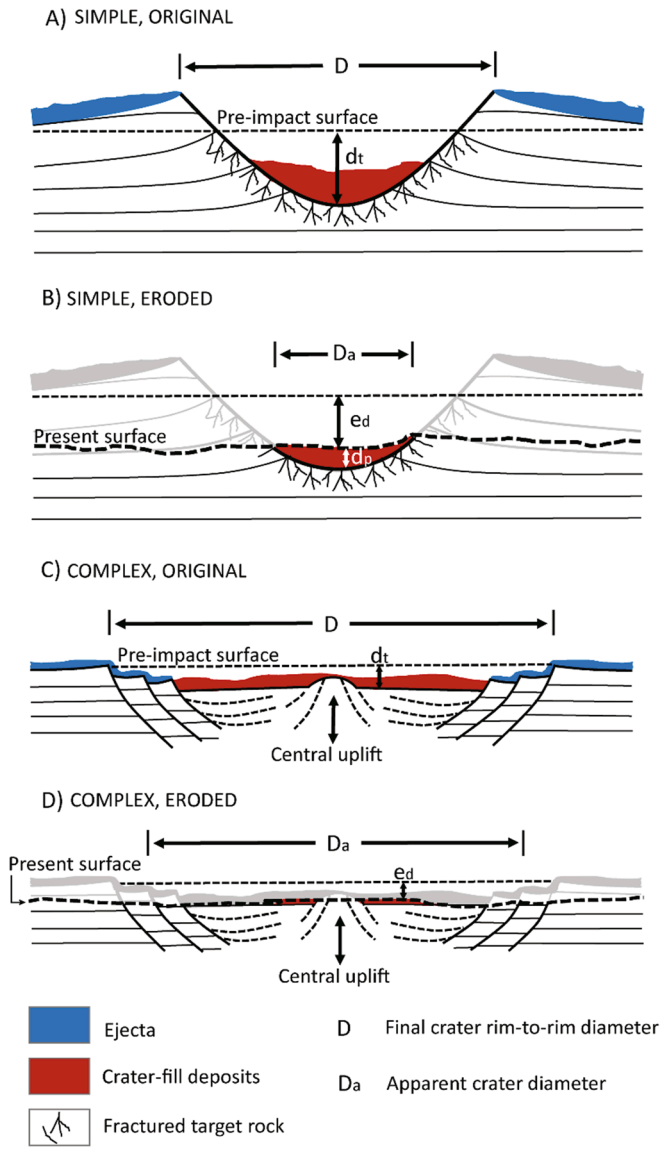

Fig. 5. Schematic models for simple and complex impact structures (Table 1) used to estimate post-impact erosion depths. Adapted from several sources (Degeai and Peulvast, 2006; Osinski et al., 2018; Peulvast et al., 2009; Turtle et al., 2005).

appears incompatible with estimated depths of late Mesoproterozoic erosion.

Any Sveconorwegian foreland basin sediment appears to have been removed early in the Mesoproterozoic. Fracture fills of sedimentary clay and quartz sands, deposited in a shallow marine environment, are found today at 60 m depth in Palaeoproterozoic crystalline rocks near Helsinki. Illite clay minerals have yielded K-Ar ages of 967–947 Ma (Elminen et al., 2018). Basement was exposed prior to this date and its surface represents U1c. Elevation differences between U1a, U1b, U1c, U2 and UQ along the northern shore of the Gulf of Finland together amount to <100 m.

4.2. Neoproterozoic

There is limited evidence for renewed burial of the shield in the early Neoproterozoic in Finland. A long depositional hiatus is found (i) in the Bothnian Bay between the Mesoproterozoic Muhos Formation (~1.3 Ga) and the late Neoproterozoic (post-650 Ma) or Early Cambrian Hailuoto Formation (Hanski et al., 2019), (ii) in the Bothnian Sea, where Early Cambrian strata rest on U1b (Winterhalter, 1972) and (iii) in the Ladoga basin between deposition of Mesoproterozoic sandstones and upper Vendian/Ediacaran sediments (Ivleva et al., 2018). The informal Söderarm Formation in the Åland Sea may include "Riphean" sandstones and shales from the early Neoproterozoic but samples are derived mainly from glacial erratics of uncertain context and age (Hagenfeldt, 1995; Söderberg and Hagenfeldt, 1995). The situation in Finland differs from southern Sweden, where the Neoproterozoic Visingsö Formation (780–730 Ma) occurs in faulted basins (Pulsipher and Dehler, 2019; Wickström and Stephens, 2020). The absence of IMPs between 1151 and >710 Ma supports the former existence of protective sedimentary covers in southern Finland during this period, perhaps including transient sedimentary cover derived from the Sveconorwegian orogenic belt. This former cover may not have been thick; an estimated thickness of sedimentary rock of ≥640 m was sufficient to protect the basement from any impact where D was ≤10 km (Table 2).

Late Ediacaran to Early Cambrian strata rest on basement south of the Gulf of Finland and in north-west Russia (Fig. 1A). Detritus derived from Precambrian basement and rapakivi granites is abundant in sedimentary rocks of similar age in Estonia (Isozaki et al., 2014). At the Lappajärvi IMP, microfossil assemblages in target rocks regarded previously as pre-Cambrian (Uutela, 1990) are now recognised as Early Cambrian in age (Slater and Willman, 2019). A similar reassessment may be necessary at the Iso-Naakkima IMP where available microfossil evidence indicates that the 100 m-thick sediment sequence is of pre-Cambrian age. The sequence is interpreted as post-impact in origin (Sarapää, 1996), with its youngest microfossils identified as Early Ediacaran (~640 Ma) (Elo et al., 1993). Alternatively, if the youngest sediment is of pre-impact age then its survival and the continued existence of this small crater can be accounted for by slow erosion in the Ediacaran and later burial. Impact melt composition at the Sääksjärvi IMP indicates that, at the time of impact at ~608 Ma (Kenny et al., 2020), a Jotnian sandstone cover persisted E of the Satakunta basin (Mutanen, 1979). In western Finland, clasts of Mesoproterozoic sandstone in Early Cambrian basal conglomerates require the persistence of older cover around Lauhanvuori (Fig. 4). The absence of Mesoproterozoic sandstone beneath the Lauhanvuori Early Cambrian outlier and beneath Early Cambrian shales in the Söderfjärden and Lappajärvi IMPs suggests, however, the widespread removal of Proterozoic sedimentary cover from western Finland by the late Neoproterozoic. Available evidence indicates that the basement in southern Finland was widely exposed in the late Neoproterozoic, with persistence of patches of Mesoproterozoic sedimentary cover.

Limited constraints are available on the depth of Cryogenian and Ediacaran erosion. The survival of the small (D = 3.8 km) IMP at Suvasvesi North dated to >710 Ma (Schmieder et al., 2016b) implies limited basement erosion during or since the Neoproterozoic. The Jänisjärvi IMP is dated to 687 ± 5 Ma and retains fragments of Neoproterozoic siltstone in its impact breccias (Jourdan et al., 2012). d_p is uncertain; hence d_t provides only a maximum depth of erosion of 650 m (Table 2). Of this total, an estimated 200 m of rock is missing below U2 due to Phanerozoic erosion (Koistinen, 1996). Late Neoproterozoic kimberlite diatremes at Kuopio in eastern Finland are dated to 620–585 Ma (Dalton et al., 2020; O'Brien, 2015). Erosion has removed kimberlite crater facies and comparisons with kimberlite pipe models (Stanley et al., 2013) indicate removal of 250–500 m of crater facies after emplacement. Kimberlite-related volcaniclastic breccias have quartzite, gneiss and granitoid clasts but lack sedimentary fragments at Kuopio (O'Brien and Tynni, 1998) and further N at Kuusamo (Dalton et al., 2019), suggesting an absence of sedimentary cover in these areas at the time of eruption. The Alnö carbonatite pipe in eastern Sweden was emplaced at 584 Ma (Meert et al., 2007) and estimated originally to have stood <500 m below the surrounding landsurface (Hall et al., 2019a). Available evidence suggests that <450 m of basement and cover was removed from southern Finland and its surroundings through the late Neoproterozoic.

4.3. Palaeozoic

The Neoproterozoic erosion phase culminated in the formation of U2 across Baltica (Fig. 1A). The extent of U2, its low relief and the lateral uniformity of its thin sedimentary cover are features that mark out U2 as one of Earth's great unconformities. U2 provides a fundamental reference surface in Fennoscandia for understanding Phanerozoic tectonics and faulting, Mesozoic and Cenozoic weathering and erosion and Pleistocene glacial erosion (Gabrielsen et al., 2015; Lidmar-Bergström and Olvmo, 2015).

In Finland, U2 is cut mainly in Archaean to Palaeoproterozoic basement (Fig. 1A). U2 is deeply and intensely weathered beneath Late Ediacaran cover along the Gulf of Finland (Liivamägi et al., 2014; Puura et al., 1996). Late Neoproterozoic to Early Palaeozoic sedimentary target rocks in the IMPs at Lappajärvi and Iso-Naakkima (Sarapää, 1996) also rest on deeply weathered rock and may indicate a formerly wider extent of Late Neoproterozoic weathering in Finland. However, in eastern and southern Sweden, deep weathering is not recorded on U2; either deep weathering profiles did not develop here before the Early Cambrian transgression or weathering mantles were removed during the transgression (Hall et al., 2019a, 2019b). Large parts of U2 show remarkably low relief (Rudberg, 1970), apart from occasional, widely-spaced ridges and inselbergs (Lidmar-Bergström, 1988). A near-monoclinal form allows linear projection of U2 in bedrock profiles (Fig. 3).

U2 is a diachronous palaeo-surface, emerging from beneath Late Ediacaran sandstones south of the Gulf of Finland, Early Cambrian sandstones in the Gulf of Bothnia and Early Ordovician limestones in eastern Sweden (Hall et al., 2019a). Sandstone dykes, dated by fossils to the Early Cambrian, Late Cambrian and Early Ordovician on Åland (Tynni, 1982), are found widely in south-west Finland (Fig. 1B), along with cavity fillings in pre-Cambrian metamorphosed limestone (Simonen, 1960). The planar form of U2 is inherited in the present basement surface on the western and eastern flanks of the SFD (Tanner, 1938) where the projected plane of U2 rises at gradients of 0.2–0.4% (Fig. 3). U2 reaches an elevation of 160 m in western Finland below the small outlier of Lower Cambrian quartz sandstone at Lauhanvuori (Söderman et al., 1983) (Fig. 4). On the crest of the SFD, U2 is cross-cut by a Cenozoic epigene erosion surface (U4: Fig. 3).

The onset of marine transgression in the Late Ediacaran led to the eventual burial of the basement to depths of 250–400 m in Estonia (Kirsimäe et al., 1999) and >200 m in the Bothnian Sea (Winterhalter et al., 1981) by the end of the Ordovician. The lateral extent and facies continuity within the near horizontal strata that comprise the Early Palaeozoic succession is remarkable and, in large part, a response to the flatness of U2 during transgression (Nielsen and Schovsbo, 2011, 2015). IMPs at Lappajärvi, Söderfjärden, Lumparn and Saarijärvi in Finland, Tvären Bay in eastern Sweden and Kärdla in Estonia hold pre- and post-impact Cambrian and Ordovician sedimentary rocks (Table 1). A $^{40}Ar/^{39}Ar$ age of 640 Ma or older for the Söderfjärden IMP (Schmieder et al., 2014) is likely too old. This IMP is infilled by Early Cambrian shale (Lehtovaara, 1982) and a 55 m-high crater rim is largely preserved (Abels et al., 2000); the rim was likely preserved by burial soon after impact at 550–530 Ma. The presence of a cluster of Early Palaeozoic IMPs on the craton surface in Fennoscandia is a product of the >100 Ma long period when U2 and its thin Early Palaeozoic cover were exposed to impacts below shallow seas, and of burial through much of the later Phanerozoic (Puura and Plado, 2005). Other clusters of preserved IMPs on shields in Australia (Haines, 2005) and North America (Schmieder et al., 2015) also have been linked to impacts on extensive, slowly-eroding surfaces, preserved as late Proterozoic to early Palaeozoic unconformities by late Palaeozoic and Mesozoic burial.

Further burial of the craton occurred from the Silurian onwards, as debris from the Caledonian orogenic belt was transported east and south-east. The main locus for sedimentation was the central part of the southern Baltic basin (Šliaupa and Hoth, 2011). In south-west Finland, hydrothermal fluorite-calcite-galena veins now exposed on U2 were likely emplaced below former Palaeozoic cover (Alm et al., 2005). Transport of Caledonian detritus further east in Finland was, however, limited. Detrital zircons of Caledonian age and provenance are sparse in Devonian sediments in Estonia (Kuznetsov et al., 2011) and the Ladoga basin (Miller et al., 2011). South of Lake Onega, Late Devonian sandstones rest directly on Late Ediacaran cover; any earlier Palaeozoic sedimentary rocks were removed before ~385 Ma. Heavy mineralogy and geochemistry indicate derivation of Late Devonian sandstones from first-cycle sources in exposed Svecofennian basement and rapakivi granites lying to the west (Terekhov et al., 2017). Available evidence indicates that Caledonian foreland basin sediments thinned eastward across Finland and did not extend into the Onega region of Russia.

Palaeozoic strata in Estonia accumulated to a maximum thickness of 0.8–1.0 km (Kirsimäe et al., 1999) in the Permian (Preeden et al., 2009). Present-day thicknesses of Palaeozoic sedimentary cover are 0.5–0.8 km (Poprawa et al., 1999) and indicate post-Permian denudation of 200–300 m of cover. For the early Carboniferous IMP at Mishina Gora, south-east of the Gulf of Finland, d_t is estimated at 220 m; this constrains the maximum post-impact depth of erosion in missing Devonian-Carboniferous sedimentary cover. As the present sedimentary sequence has a thickness of 460–530 m (Masaitis, 1999) then the total thickness of the Palaeozoic cover at the time of impact was <680–750 m. Limited burial is supported by minor illite diagenesis in Early Cambrian clays in Estonia (Kirsimäe et al., 1999)

Early Palaeozoic sedimentary rock units decrease in thickness northward across Estonia towards Finland (Poprawa et al., 1999). Maximum burial temperatures of <35–50 °C in Finland are indicated by (i) acritarch colour-alteration in Early Cambrian clays and sandstones in Finland at the Lappajärvi IMP (Slater and Willman, 2019), similar to Estonia (Talyzina, 1998), and (ii) limited thermal alteration of Cambrian and perhaps older microfossils in the Iso-Naakkima IMP (Elo et al., 1993). The maximum former thickness of Palaeozoic sedimentary cover at sites across southern Finland was <0.68–1.0 km. IMPs are not recognised in Finland during the interval 510–245 Ma (Table 1), consistent with protection of the basement surface beneath cover rocks.

4.4. Mesozoic

Important inferences about the distribution and thickness of sedimentary cover and depths of erosion in basement and cover through the Mesozoic may be derived from IMPs in southern Finland. Two IMPs of Triassic age are known: Karikkoselkä (Schmieder et al., 2010; Schwarz et al., 2015) and Paasselkä (Schwarz et al., 2015). Two IMPs date from the Late Cretaceous: Lappajärvi (Schmieder and Jourdan, 2013) and Suvasvesi North (Schmieder et al., 2016b) (Table 1). The Karikkoselkä and Lappajärvi impact targets each retained Early Cambrian to Middle Ordovician sedimentary cover at the time of impact (Pesonen et al., 1999; Schmieder et al., 2008; Slater and Willman, 2019). Siltstone and sandstone fragments of unknown age are recorded from impact breccias at Paasselkä (Abels et al., 2002; Buchner et al., 2009). In contrast, no pre- or post-impact sedimentary cover rocks are known from the IMP at Suvasvesi North (Pesonen et al., 1999; Werner et al., 2002). Similarly, the target for the Early Cretaceous IMP at Dellen, eastern Sweden, was likely the exposed basement (Mark et al., 2014). The sedimentary rocks preserved in IMPs indicate that (i) western and southern Finland retained Early Palaeozoic cover through the Mesozoic, whereas (ii) in eastern Finland, Early Palaeozoic cover persisted in the Triassic, but the basement was re-exposed by the Late Cretaceous.

The original depths of the two Triassic IMPS constrain the maximum remaining depths of Palaeozoic sedimentary rock at the time of impact to 170–490 m (Table 2). As the original thickness of Early Palaeozoic cover in Estonia amounted to 250–400 m (Kirsimäe et al., 1999), the remaining Late Palaeozoic sedimentary cover in southern Finland was already thin by the Triassic. Significant thinning of Late Palaeozoic and older cover rocks likely occurred during Permian epeirogenic uplift; when fault and shear zones were reactivated in southern Finland

(Preeden et al., 2009).

At the Lappajärvi IMP, the Palaeozoic sedimentary overburden had been reduced to a thickness to ~170 m by the time of impact at 78 Ma. No traces of pre-existing Mesozoic sedimentary rocks are reported from the Cretaceous IMPs; there was no thick Mesozoic sedimentary cover on this part of the shield. The Triassic and Late Cretaceous impacts were separated in time by ~160 Ma but today the IMPs remain at similar elevations (100–130 m a. s. l.). Post-impact erosion depths for Mesozoic IMPs are estimated at <250 m in basement and cover (Table 1), similar to the estimate for the Late Cretaceous Lappajärvi IMP. Hence, Mesozoic erosion was limited in its depth and confined mainly to older sedimentary cover. Unlike in southern Sweden (Lidmar-Bergström et al., 1997), the basement in south-western Finland remained protected from Mesozoic deep weathering beneath sedimentary cover. Low erosion rates indicate little, if any uplift of southern Finland in the Mesozoic.

4.5. Cenozoic

No IMPs of Cenozoic age are known in Finland. Post-impact erosion depths at Lappajärvi constrain Cenozoic erosion depths in that part of western Finland. The inclined surface of U2 defines the flanks of the SFD (Fig. 1A). Projections indicate that erosion in basement increased northwards from the Gulf of Finland. On the crest of the SFD, the depth of missing basement is 100–200 m, roughly equivalent to post-impact erosion depth at Lappajärvi. A Cenozoic planation surface, U4, cross-cuts U2 (Fig. 3). This surface rises slightly above 200 m a.s.l. and is inclined gently south-eastward. U4 carries kaolinitic deep weathering with D/H and $^{18}O/^{16}O$ ratios consistent with formation at temperatures of 13–15 °C, similar to Eocene and Miocene palaeotemperatures at 60–70° N (Gilg et al., 2013). Alternatively, the Litmanen kaolin in south-central Finland has yielded previously three K–Ar dates of 1189 ± 18 to 1151 ± 22 Ma for subsidiary illites (Sarapää, 1996). Whilst these dates are consistent with inheritance of weathering from U1b, survival of the weathering requires near-zero erosion depths in the late Mesoproterozoic and Neoproterozoic, a scenario which is inconsistent with the erosion and burial history presented here. Geochemically-immature sandy weathering covers are reported on U4 in eastern and northern Finland (Hall et al., 2015) and indicate that the final shaping of U4 was likely under humid temperate conditions in the Neogene.

The preservation of U2 on the flanks of the SFD requires geologically-recent re-exposure. Losses of several tens of metres of Early Palaeozoic sedimentary rock from U2 around the Baltic Sea Basin have been attributed to erosion beneath Pleistocene ice sheets since 1.2 Ma (Hall and van Boeckel, 2020). This erosion may have included the re-exposure

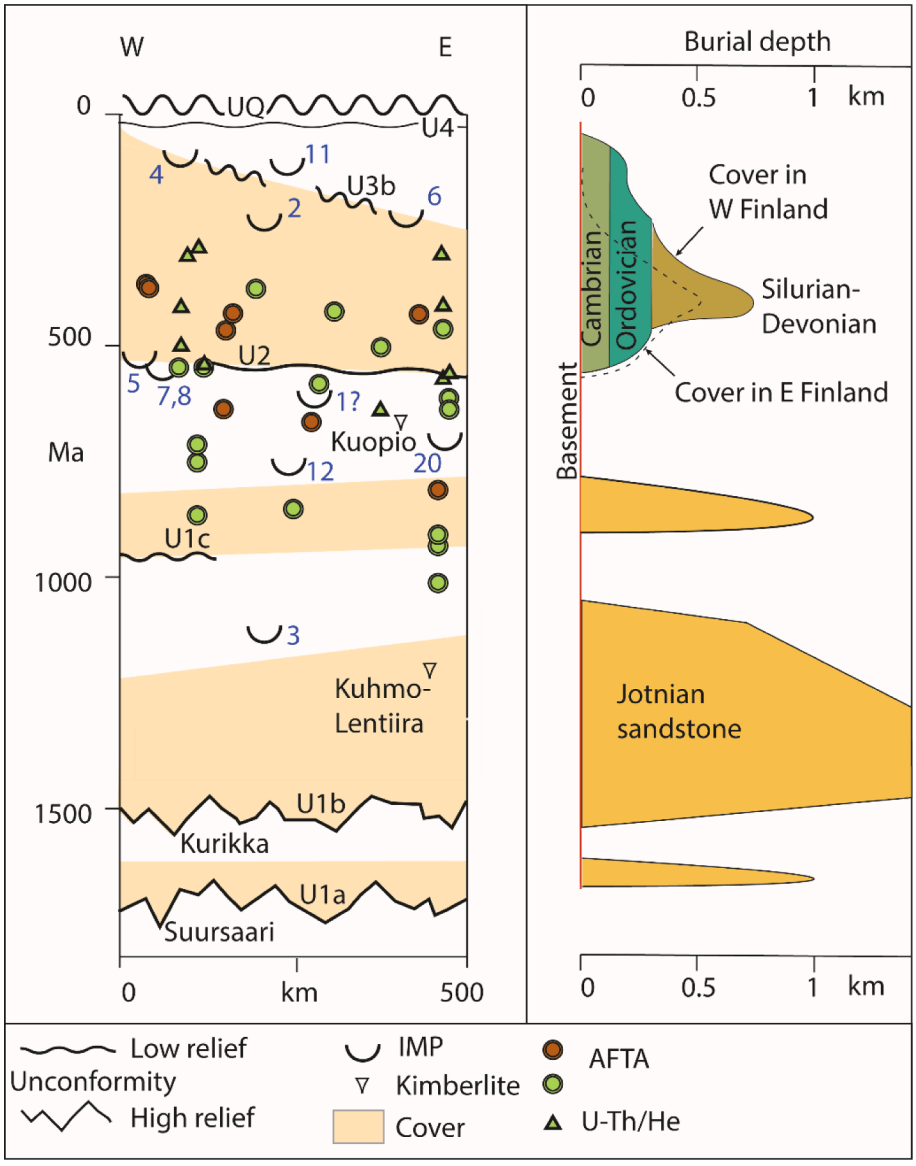

Fig. 6. Low temperature thermochronology and the erosion and burial history of southern Finland. Unconformities, impact structures and cooling ages from published thermochronology. Data from Murrell and Andriessen (2004) (red) and Kohn et al. (2009) (green). Pale brown shading denotes periods with burial of basement from W to E across southern Finland. Schematic post-1.7 Ga burial and erosion curve. (For interpretation of the references to colour in this figure legend, the reader is referred to the web version of this article.)

of the well-preserved crater at Söderfjärden (Fig. 1B). On the crest of the SFD, the FIS modified and locally reshaped basement surfaces, for example in the Finnish Lake District (Punkari, 1994), mainly through the removal of saprolite, forming a new unconformity, UQ, presently buried by unconsolidated Quaternary sediments.

5. Comparisons with low-temperature thermochronology

Low-temperature thermochronology (LTT) is an important tool for assessing erosion and burial histories on cratons (Kohn and Gleadow, 2019). Published apatite fission track (AFT) and (U–Th)/He apparent cooling ages for Finland range from 1027 Ma to 240 Ma (Fig. 6) and include some of the oldest ages recorded from any craton on Earth (Hendriks et al., 2007; Kohn et al., 2009; Murrell and Andriessen, 2004). The dataset supports prolonged residence in the AFT partial annealing zone (PAZ) at ~60–110 °C and the (U-Th/He) partial resetting zone (PRZ) at ~35–85 °C (Kohn and Gleadow, 2019), consistent with slow erosion of the craton surface since 1 Ga. The AFT dataset for Finland, however, shows significant scatter in ages between sample locations over short distances, reaching up to 650 Ma in eastern Finland (Fig. 6). Moreover, (U-Th)/He ages always should be younger than paired AFT ages due to lower cooling temperatures, but this is often not the case in Finland (Hendriks and Redfield, 2005). Several reasons have been suggested for such differences in similar settings which include (i) variations in apatite chemistry, especially for gabbros, in which apatites usually display higher Cl content coupled with the oldest AFT ages (Kohn et al., 2009), (ii) differences in heat flow, rock conductivity or heat production (Łuszczak et al., 2017; Veikkolainen and Kukkonen, 2019) and (iii) the effects of α-radiation-enhanced annealing (Hendriks and Redfield, 2005).

Notwithstanding these uncertainties, models based on LTT data have been used to develop detailed models of the cooling history of the craton in Finland. Neoproterozoic AFT ages have been related to removal of a former Sveconorwegian foreland section, several km thick, which had earlier totally reset fission tracks (Murrell and Andriessen, 2004). AFT cooling ages between 830 and 600 Ma have been linked to deep erosion that led to the formation of U2 (Murrell and Andriessen, 2004). Thermal modelling of AFT data from three ~1 km deep drill holes across southern Finland has provided estimates that sedimentary detritus derived from the Caledonian orogenic belt had buried most of Finland to depths of 0.5–1.5 km (Larson et al., 1999) or 3 km by the Devonian (Murrell and Andriessen, 2004). A phase of Palaeocene cooling is also recognised but remains poorly constrained (Murrell and Andriessen, 2004). (U-Th)/He thermochronology, however, presents a different scenario in east-central Sweden. Surface samples at Forsmark cooled below 70 °C between 750 and 530 Ma during the formation of U2 and were not reheated thereafter, with a slow exhumation at 2 m/Ma between 500 and 250 Ma (Page et al., 2007). More generally, LTT data from southern Finland has been interpreted as evidence for episodic km-scale burial and erosion of sedimentary cover and as an example of a tectonically and topographically dynamic craton (Kohn and Gleadow, 2019).

Regionally extensive unconformities are key time markers for interpretation of crustal temperature histories (Gunnell et al., 2007; Japsen et al., 2016; Zapata et al., 2019). On the shield in Finland, unconformities represent different periods when cooling of rocks on unconformities approached ambient surface temperatures. U1c to U4 formed after the cessation of significant magmatic activity on the craton. Hence, any later resetting requires deep burial by sedimentary rocks. Heating above 60–80 °C, a minimum for resetting apatite fission tracks, requires burial by >4 km of overburden at modern geothermal gradients in Finland of 8–14 °C/km (Kukkonen and Lahtinen, 2001). U2, formed by ~550 Ma, is a key datum due to its extent, near-planar form and minor dislocation by later faulting (Puura et al., 1996). Effectively, all basement rocks come from 0 to 200 m below U2 (Fig. 3). Hence, the LTT samples in southern Finland share a common cooling history from the Late Neoproterozoic onwards.

U1b formed at ~1.5 Ga but it is not represented by AFT ages in southern Finland despite standing at a similar erosional level to U2 and younger basement unconformities (Fig. 3). Whilst this non-representation may be attributed locally to Mesoproterozoic reheating by granite and dyke intrusion, large areas of southern Finland are remote from such intrusions (Fig. 1B). Moreover, resetting by Mesoproterozoic and later deep burial appears unlikely as the total thickness of sedimentary overburden and Postjotnian diabases removed since the Mesoproterozoic is estimated to have reached only 0.5–2.0 km outside Jotnian basins (Puura et al., 1996). Erosion depth indicators formed before the Sveconorwegian Orogeny, namely the IMP at Keurusselkä (Raiskila et al., 2011) and the kimberlite dykes at Kuhmo (Dalton et al., 2020), suggest 0.8–1.2 km of rock loss after 1.2 Ga. The illite clays on U1c in southern Finland are equivalent in age to the later phases of the Sveconorwegian Orogeny. The clays were deposited in a shallow marine basin and lack diagenetic overprinting (Elminen et al., 2018), consistent with shallow burial of the basement in the early Neoproterozoic and later. There is presently little independent evidence for burial to depths of >4 km necessary to reset apatite fission tracks after formation of U1b and U1c.

U2 represents the culmination of Neoproterozoic erosion after formation of U1c and its burial. The absence of IMPs dated to 1151 to >720 Ma is consistent with protection of basement by thin sedimentary cover. Estimated erosion depths between 680 and 550 Ma amounted to <500–650 m. Reported LTT cooling ages are scattered throughout the Neoproterozoic (Fig. 6). Simple cooling requires removal of sedimentary cover because U1c and U2 remain at a similar erosion level in the basement. Modelled cooling from ~110 °C at ~830 Ma, passing through the upper limit of the partial annealing zone (PAZ) at ≥60 °C at ~600 Ma requires overburden thicknesses of 3–5–5 km at present geothermal gradients (Murrell and Andriessen, 2004). This scenario is problematic as (i) evidence is lacking for burial of U1c to depths >1 km in and after the Neoproterozoic, (ii) closely-spaced localities apparently passed through the PAZ at widely different times in terrain without evidence of differential tectonics and (iii) rocks in southern Finland passed through the PAZ long before 680 Ma and probably before the formation of U1c.

Few reported LTT ages correspond with the onset of burial of U2 at 550 Ma, consistent with rock cooling before the final stages of its formation. Cooling ages between 527 and 426 Ma, however, are anomalous in being younger than U2. A possible explanation is that these rocks were reheated beneath Caledonian foreland basin sediments but to temperatures below the 110 °C necessary for complete resetting (Larson et al., 1999). However, the former overburden thicknesses of 0.5–1.5 km (Larson et al., 1999) or 3 km (Murrell and Andriessen, 2004) modelled using LTT for these sediments in Finland are at the upper end or above the <0.68–1.0 km thicknesses suggested by unconformities, IMPs and other geological indicators.

Similar overestimation of former sedimentary cover thickness may apply across the axis across the former Caledonian foreland basin to the west. AFT models have provided estimates of overburden thicknesses at >2.5 km, and reaching 4 km (Larson et al., 2006), or 6 km (Samuelsson and Middleton, 1998) over a 300–600 km wide swath in western and southern Sweden, but these estimates remain controversial (Hendriks and Redfield, 2005, 2006) and are much greater than the thicknesses of sedimentary cover estimated in this study for southern Finland. A critical constraint is provided by the Siljan IMP (Fig. 1A), the largest in western Europe. The Siljan impact is dated to the Early Devonian (~400 Ma; (Jourdan et al., 2012), during the Caledonian orogeny (~420–350 Ma). The impact target included Silurian to Early Devonian sedimentary rocks that are preserved within the Siljan IMP (Juhlin et al., 2012). Application of the empirical relationship used for IMPs in Finland to the Siljan impact is not straightforward due to the poor constraints on D (53–91 km; (Holm et al., 2011)) and d_t (>0.6 km; (Holm et al., 2011)) at Siljan but the estimated rock thicknesses lost to post-impact erosion are up to 680–1140 m. The total stratigraphic thickness for the Cambrian to Early Devonian cover preserved within the Siljan structure has been

estimated as >460–500 m (Juhlin et al., 2012). Assuming this thickness was typical for the surrounding basement at the time of impact, accumulation of further sedimentary cover in the late Palaeozoic was restricted to a maximum thickness of 220–680 m. Despite significant uncertainties, the preserved thicknesses of sedimentary cover at Siljan and the estimated depths of rock removed by erosion since the Siljan impact indicate that the Caledonian foreland basin in west-central Sweden was significantly shallower than previously suggested.

Two important differences emerge when LTT scenarios for Finland are compared to other geological evidence. Firstly, Proterozoic unconformities are not clearly represented in LTT models despite post-formational maximum burial depths of <1 km. Secondly, the apparent thickness of former overburden is overestimated in AFT models. Sedimentary overburden thicknesses were far below the 4 km depths necessary for resetting of apatite fission tracks. For Proterozoic unconformities in Finland, overestimation is by a factor of 4; for U2, overestimation is by a factor of 2 or more.

6. Discussion

6.1. Tiered unconformities

The sequence and timing of erosion and burial indicated by unconformities, IMPs and other geological proxies in this study generally conforms to previous reconstructions of the geological history and position of the shield in Finland (Kohonen and Rämö, 2005) from the Mesoproterozoic onwards (Fig. 2). The main uncertainties in the timing of events relate to the ages of sedimentary outliers, particularly non-fossiliferous sandstones, and IMPs that currently lack secure dating (IMPs 1, 10 and 12). U1b, the sub-Jotnian unconformity (Lundmark and Lamminen, 2016), and U2, the sub-Ediacaran to sub-Ordovician unconformity (Lidmar-Bergström, 1993; Lidmar-Bergström and Olvmo, 2015), are found widely across Fennoscandia (Fig. 1A). The early Proterozoic unconformity, U1a (Pokki et al., 2013b), and the early Neoproterozoic unconformity, U1c (Elminen et al., 2018), appear to be of more regional significance. Triassic to Jurassic (U3a) and Late Cretaceous (U3b) unconformities found in southernmost Sweden (Japsen et al., 2016) are not clearly represented in southern Finland, likely due to the later persistence here of Early Palaeozoic cover rocks. U4 developed after re-exposure of basement on the SFD and so is broadly equivalent to etchsurfaces recognised across Fennoscandia that were initiated in the Late Cretaceous and that continued to develop by weathering and erosion in response to uplift, doming and tilting through the Palaeogene and Neogene (Ebert et al., 2011; Lidmar-Bergström, 1995; Lidmar-Bergström and Olvmo, 2015). Quaternary glacial erosion shaped the youngest unconformity (UQ) and represents a brief but significant erosional phase (Hall and van Boeckel, 2020).

Tiered basement unconformities of widely different ages are typical of many of the Earth's shields and platforms. Craton surfaces in Western and South Australia carry exhumed and buried Neoproterozoic, Late Cambrian and Late Palaeozoic unconformities (Baillie et al., 1994; Eyles and de Broekert, 2001) and exhumed early Mesozoic planation surfaces and later Cretaceous to Palaeogene epigene planation surfaces (Twidale, 2000; Twidale et al., 2020). On parts of Laurentia, now in North America, the unconformity stack includes the continent-wide, sub-Ordovician "Great Unconformity" (Peters and Gaines, 2012), the sub-Carboniferous unconformity in eastern Canada (Peulvast et al., 1996) and the exhumed sub-Eocene and epigene Neogene surfaces in the Canadian Arctic (Bird, 1967). On the fragment of Laurentia in north-west Scotland, the stack includes sub-Torridonian (Stewart, 1972), sub-Cambrian (Parnell et al., 2014) and sub-Triassic unconformities and younger epigene surfaces (Godard, 1965). On the Neoproterozoic basement platform in north-east Scotland, tiered unconformities include sub-Devonian, sub-Triassic and sub-late Cretaceous palaeosurfaces (Hall, 1991). On the Variscan platform in Brittany, France, six separate post-191 Ma planation surfaces are recognised, with the older unconformities exhumed after two phases of burial in the Jurassic and Late Cretaceous (Bessin et al., 2015). Post-Triassic erosion on the granite batholith of SW England has been similarly limited in depth below the sub-Triassic unconformity (Gunnell, 2020). Tiered basement unconformities indicate that, in common with the craton in Finland, these shields and platforms experienced multiple mega-cycles of uplift, limited denudation close to base level and burial.

6.2. Ultra-slow cratonic erosion

Tiered basement unconformities U1 to U4 span 1.5 Ga yet differ in elevation by 0–200 m from the present land surface. Average erosion rates in basement were near zero in areas, like Kurikka, where U1b and U2 are preserved in the present topography. Over a similar period of the Proterozoic, average exhumation rates on Kola were 1–2 m/Ma (Veselovskiy et al., 2019). In eastern Finland and at Alnö, Sweden, maximum average erosion rates in basement since ~580 Ma were <1 m/Ma. On the crest of the SFD (Fig. 3), projections of U2 indicate that up to 200 m of basement is missing since exhumation in the Late Cretaceous, representing a maximum average erosion rate of 2.5 m/Ma. The former Palaeozoic sedimentary cover across southern Finland reached its maximum thickness of 0.68–1.0 km in the Permian and was eroded thereafter at average rates of 2–4 m/Ma. On the Kola peninsula, north-west Russia, sedimentary outliers and kimberlite and carbonatite intrusions constrain average post-Devonian erosion rates in basement and cover to similar rates of <3–6 m/Ma (Hall, 2015). At Lappajärvi, an estimated 170 m of sedimentary cover has been removed from the IMP since 78 Ma, an average erosion rate of 2.2 m/Ma (Table 2). The pre-Cenozoic averages include long periods of zero erosion during burial and mask episodically slightly higher rates during periods of minor uplift (Fig. 6).

Erosion rates on other craton surfaces are starting to be documented. On the western Canadian shield, AHe thermochronology indicates erosion rates in basement of ≤2.5 m/Ma since 1.7 Ga (Flowers et al., 2006). Similar erosion rates since 1.5 Ga are indicated by U-Pb thermochronology on volcanically exhumed lower crustal fragments in Montana, USA (Blackburn et al., 2012). On the eastern and northern Canadian shield, Phanerozoic erosion rates in basement and cover derived from IMPs are 2–8 m/Ma (Peulvast et al., 2009). Typical Cenozoic erosion rates on cratons derived from geological, geomorphological and dating evidence are 2–20 m/Ma (Beauvais et al., 2016; Beauvais and Chardon, 2013; Vasconcelos and Carmo, 2018). Hence, whilst average rates of erosion on the craton on southern Finland are ultra-slow, and amongst the lowest reported on Earth, they are comparable to other cratons.

6.3. Persistence of other geological markers for slow erosion

Limited depths of long-term erosion in basement can account for several distinctive geological features of the craton. Fracture sets generated through brittle deformation in western Finland and eastern Sweden at ~1.7 Ga carry multiple generations of Proterozoic and younger mineral coatings (Blyth et al., 2000, 2004; Drake et al., 2020; Karhu, 2000). Phanerozoic mineral coatings indicate phases of fracture reactivation and fluid circulation at depths of up to 1 km in response to far-field tectonic forces (Saintot et al., 2011), Permian magmatism (Holm et al., 2010), and burial by sedimentary cover (Drake et al., 2020; Sandström and Tullborg, 2009). The preservation of Early Cambrian sandstone dykes formed on U2 (Friese et al., 2011) and mineral coatings in basement fractures derived from former Early Palaeozoic cover, such as asphaltite derived from Alum Shale (Sandström et al., 2006) and calcite formed after dissolution of Ordovician limestones (Hall et al., 2019a) provide evidence of geologically-recent re-exposure of basement on U2. Low Cenozoic erosion rates across Finland are consistent with the widespread preservation of Palaeogene and Neogene saprolite (Gilg et al., 2013; Hall et al., 2015; Perttunen, 1970; Vartiainen, 1980) and

associated supergene mineralisation (Tuisku, 2010). Slow erosion has also allowed the survival of Palaeogene deep groundwater and its associated microbiomes in western Finland (Kietäväinen et al., 2014; Rajala et al., 2015) and eastern Sweden (Drake et al., 2018). In less stable settings, similar subsurface markers for slow cratonic change were erased by Phanerozoic erosion.

6.4. Challenges for low temperature thermochronology in cratonic settings

LTT has become a standard tool for estimating integrated long-term denudation rates on cratons. Interpretations based on thermochronology often invoke craton burial by sedimentary rocks several km-thick to account for Phanerozoic cooling ages (Japsen et al., 2016; Kohn and Gleadow, 2019). Large parts of Finland were covered by sediment derived from erosion of the Sveconorwegian and Caledonian orogenic belts. The geometries of IMPs, diagenetic effects and stratal thicknesses south of the Gulf of Finland indicate, however, that foreland cover thicknesses were <1 km, thinning eastward. This indicates that available AFT thermochronology in Finland overestimates overburden thickness by factors of at least 2–4.

Similar disparities exist for overburden losses when LTT is compared with other geological proxies for Phanerozoic erosion on other cratons in SE Australia (Webb, 2017), NE Brazil (Peulvast et al., 2008) and E Argentina (Demoulin et al., 2005). Large overestimates of Cenozoic erosion rates are also apparent when LTT results are compared with absolute dates for minerals in Cenozoic weathering profiles on cratons in West Africa (Beauvais and Chardon, 2013) and in Brazil (Vasconcelos and Carmo, 2018). The reasons for overestimation of denudation by LTT in such cratonic settings are unclear. Radiation damage affects both the AFT and (U-Th)/He thermochronometers in slowly-cooled settings (McDannell et al., 2019). Burial leads to enhanced heat retention and flow beneath cover rocks (Łuszczak et al., 2017). On the Gawler Craton, South Australia, AFT and U–Th–Sm/He data have yielded a range of apparent single grain ages across samples and within individual samples (Reddy et al., 2015) on a craton with multiple tiered unconformities that was buried for long intervals after first exposure in the Mesoproterozoic (Twidale et al., 2020). AFT data provide evidence for Late Cretaceous-early Palaeogene thermal refraction driven by circulation of heated (~60–110 °C) groundwater beneath the former sedimentary cover of the Eromanga Basin aquifer system (Boone et al., 2016). On these cratons and platforms, long residence times within the PAZ and PRZ have led to pervasive, subtle but little understood effects on the kinetics of annealing and diffusion.

In southern Finland, the surface of the craton has remained close to its present erosion level since 1.5 Ga; the residence time for rocks at or below PAZ and PRZ temperatures is long. Sedimentary cover provided a <1 km-thick insulating blanket to the craton for much of Proterozoic and Phanerozoic. Evidence for widespread thermal refraction at temperatures of 60 to 200 °C (but mainly <100 °C) below former Phanerozoic sedimentary cover is provided by mineral coatings on basement fracture surfaces in south-western Finland (Sahlstedt et al., 2013) and eastern Sweden (Sandström and Tullborg, 2009) and by calcite–-sphalerite veins in Silurian limestones in Estonia (Eensaar et al., 2017). Additionally, radiogenic heat production is spatially variable in Finland (Veikkolainen and Kukkonen, 2019) and radiation damage effects are widespread in apatites (Hendriks and Redfield, 2005; Kohn et al., 2009). Successful application of LTT models under these circumstances remains challenging. New LTT approaches may be required, including analyses of individual crystals of apatite (Fox et al., 2017). New LTT models, including emerging THe and ZHe models (Baughman and Flowers, 2020), can be tested on cratons where erosion and burial histories are relatively well-constrained by other geological proxies, as in Finland (Fig. 6).

6.5. The cratonic regime in Finland

Ultra-slow erosion of the craton in southern Finland is consistent with the tectonic and thermal stability provided by a 250–300 km deep keel of lithosphere (Artemieva, 2003). The protracted burial of southern Finland, together with the ~120 Ma duration of the Early Palaeozoic marine transgression, protected the shield surface from erosion for ~1.0 Ga (Fig. 6). The narrow elevation range of the stacked unconformities in southern Finland indicates that the episodic load on the craton from successive sedimentary covers was released after erosion through isostatic rebound and repeatedly returned the shield surface to approximately its previous erosional level. Periods of exposure, each culminating in formation of an unconformity, were relatively brief (Fig. 6). U1c and U2 were formerly covered by marine sediments, indicating an original position at base level. U4 stands only ~200 m above present sea level. There is little evidence for high relief on the craton after downwearing of the rapakivi granite intrusions at 1.5 Ga. Hence, persistent low relief has kept erosion rates low during periods of basement exposure. The shield surface in Finland provides evidence of a long evolution under a cratonic regime (Fairbridge and Finkl, 1980), where long-term tectonic stability led to ultra-slow erosion rates in basement and cover and prolonged but shallow burial.

7. Conclusions

Multiple tiered unconformities are recognised on the craton of southern Finland that formed after its stabilisation at ~1.65 Ga. Impact structures dating from 1.2 Ga had target surfaces in basement and sedimentary cover. For dated structures with impact melt rocks and breccias at known depth, the original elevation of the target surface is reconstructed, and the depth of post-impact erosion is calculated. Mesoproterozoic and younger erosion rates were ultra-slow at <2.5 m/Ma. During long periods of burial, the sedimentary overburden did not exceed ~1 km in thickness. This finding is incompatible with low-temperature thermochronology models that predict resetting of cooling ages under sedimentary cover that was several km thick following the Sveconorwegian and Caledonian orogenies. Decoupling of cooling patterns from exhumation on cratons may result from the effects of radiogenic heat production, radiation damage, insulation by sedimentary cover and circulation of heated groundwater. The cratonic regime in southern Finland involved long-term tectonic stability, prolonged but episodic shallow burial and ultra-slow erosion.

CRediT authorship contribution statement

Adrian M. Hall: Conceptualization, Methodology, Writing - original draft, Visualization. **Niko Putkinen:** Investigation, Visualization, Writing - review & editing. **Satu Hietala:** Validation, Visualization, Writing - review & editing. **Elina Lindsberg:** Validation, Visualization. **Marko Holma:** Validation, Writing - review & editing.

Declaration of Competing Interest

The authors declare that they have no known competing financial interests or personal relationships that could have appeared to influence the work reported in this paper.

Acknowledgements

This paper is built on the earlier observations and results from many geoscientists. The authors gratefully acknowledge the careful and informed critical commentary provided by the Chief Editor and three anonymous referees. Field discussions with Pasi Talvitie, Jari Nenonen and Tapani Tervo informed our understanding of the basement topography in Ostrobothnia. The draft paper benefitted from the comments on thermochronology by Fin Stuart (SUERC). This is APSI Contribution

#12.

References

Abels, A., 2003. Investigation of impact structures in Finland (Söderfjärden, Lumparn, Lappajärvi) by digital integration of multidisciplinary geodata. Westfalian-Wilhelms University, Münster, Germany.

Abels, A., Bergman, L., Lehtinen, M., Pesonen, L.J., 2000. Structural constraints and interpretations on the formation of the Söderfjärden and Lumparn impact structures, Finland [abs.]. In: Plado, J., Pesonen, L.J. (Eds.), Meteorite Impacts in Precambrian Shields. Programme and Abstracts, the 4th Workshop of the European Science Foundation Impact Programme. Geological Survey of Finland and University of Helsinki, Lappajarvi-Karikkoselka-Saaksjarvi, Finland, p. 26.

Abels, A., Mannola, P., Lehtinen, M., Bergman, L., Pesonen, L.J., 1998. New observations of the properties of the Lumparn impact structure, Åland Islands, southwestern Finland. Meteorit. Planet. Sci. Supplement 33, A7.

Abels, A., Plado, J., Pesonen, L.J., Lehtinen, M., 2002. The impact cratering record of Fennoscandia. In: Plado, J., Pesonen, L.J. (Eds.), Impacts in Precambrian Shields. Springer Verlag, pp. 1–58.

Alm, E., Huhma, H., Sundblad, K., 2005. Preliminary Palaeozoic Sm-Nd ages of fluorite-calcite-galena veins in the southeastern part of the Fennoscandian Shield. Svensk Kärnbränslehantering AB. SKB R-04-27.

Amantov, A., 1995. Plio Pleistocene Erosion of Fennoscandia and its Implications for Baltic Area. Proceedings of the Third Marine Geological Conference "The Baltic". Prace Panstwowego Instytutu Geologicznego.

André, M.-F., Peulvast, J.-P., Godard, A., Sellier, D., 2001. Landscape development in arctic, sub-arctic and circum-arctic shield environments. In: Godard, A., Lagasquie, J.-J., Lageat, Y. (Eds.), Basement regions. Springer, Berlin, pp. 199–220.

Artemieva, I.M., 2003. Lithospheric structure, composition, and thermal regime of the East European Craton: implications for the subsidence of the Russian platform. Earth Planet. Sci. Lett. 213, 431–446.

Baillie, P., Powell, C.M., Li, Z.-X., Ryall, A., 1994. The tectonic framework of Western Australia's Neoproterozoic to Recent sedimentary basins, The Sedimentary Basins of Western Australia. In: Proceedings of the Petroleum Exploration Society of Australia Symposium, p. 62.

Baughman, J.S., Flowers, R.M., 2020. Mesoproterozoic burial of the Kaapvaal craton, southern Africa during Rodinia supercontinent assembly from (U-Th)/He thermochronology. Earth Planet. Sci. Lett. 531, 115930.

Beauvais, A., Bonnet, N., Chardon, D., Arnaud, E., Arnaud, N., Jayananda, M., 2016. Very long-term stability of passive margin escarpment constrained by $^{40}Ar/^{39}Ar$ dating of K-Mn oxides. Geology 44, 299–302.

Beauvais, A., Chardon, D., 2013. Modes, tempo, and spatial variability of Cenozoic cratonic denudation: The West African example. Geochem. Geophys. Geosyst. 14, 1590–1608.

Bessin, P., Guillocheau, F., Robin, C., Schroëtter, J.-M., Bauer, H., 2015. Planation surfaces of the Armorican Massif (western France): denudation chronology of a Mesozoic land surface twice exhumed in response to relative crustal movements between Iberia and Eurasia. Geomorphology 233, 75–91.

Bird, J.B., 1967. The Physiography of Arctic Canada: With Special Reference to the Area South of Parry Channel. Johns Hopkins Press, Baltimore.

Blackburn, T.J., Bowring, S.A., Perron, J.T., Mahan, K.H., Dudas, F.O., Barnhart, K.R., 2012. An exhumation history of continents over billion-year time scales. Science 335, 73–76.

Blyth, A., Frape, S., Blomqvist, R., Nissinen, P., 2000. Assessing the past thermal and chemical history of fluids in crystalline rock by combining fluid inclusion and isotopic investigations of fracture calcite. Appl. Geochem. 15, 1417–1437.

Blyth, A., Frape, S., Ruskeeniemi, T., Blomqvist, R., 2004. Origins, closed system formation and preservation of calcites in glaciated crystalline bedrock: evidence from the Palmottu natural analogue site, Finland. Appl. Geochem. 19, 675–686.

Boone, S., Seiler, C., Reid, A., Kohn, B., Gleadow, A., 2016. An Upper Cretaceous paleo-aquifer system in the Eromanga Basin of the central Gawler Craton, South Australia: evidence from apatite fission track thermochronology. Aust. J. Earth Sci. 63, 315–331.

Buchner, E., Moilanen, J., Öhman, T., Schmieder, M., 2009. Shock-molten sandstone clasts in impact melt rocks: Age constraints for the Paasselkä impact structure (SE Finland). Lunar and Planetary Science Conference, 40. The Woodlands, Texas, p. 2169.

Buntin, S., Malehmir, A., Koyi, H., Hogdahl, K., Malinowski, M., Larsson, S.A., Thybo, H., Juhlin, C., Korja, A., Gorszczyk, A., 2019. Emplacement and 3D geometry of crustal-scale saucer-shaped intrusions in the Fennoscandian Shield. Sci. Rep. 9, 10498.

Dalton, H., Giuliani, A., O'Brien, H., Phillips, D., Hergt, J., Maas, R., 2019. Petrogenesis of a hybrid cluster of evolved kimberlites and ultramafic lamprophyres in the Kuusamo area, Finland. J. Petrol. 60, 2025–2050.

Dalton, H., Giuliani, A., Phillips, D., Hergt, J., Maas, R., Matchan, E., Woodhead, J., O'Brien, H., 2020. A comparison of geochronological methods commonly applied to kimberlites and related rocks: three case studies from Finland. Chem. Geol. 119899.

Degeai, J.-P., Peulvast, J.-P., 2006. Calcul de l'érosion à long terme en région de socle autour de grands astroblèmes du Québec et de France. Géog. Phys. Quatern. 60, 131–148.

Demoulin, A., Zarate, M., Rabassa, J., 2005. Long-term landscape development: a perspective from the southern Buenos Aires ranges of east central Argentina. J. S. Am. Earth Sci. 19, 193–204.

Donner, J., 1996. On the origin and glacial transport of erratics of Jotnian sandstone in southwestern Finland. Bull. Geol. Soc. Finland 68, 72–83.

Drake, H., Ivarsson, M., Tillberg, M., Whitehouse, M., Kooijman, E., 2018. Ancient microbial activity in deep hydraulically conductive fracture zones within the Forsmark target area for geological nuclear waste disposal, Sweden. Geosciences 8, 211.

Drake, H., Kooijman, E., Kielman-Schmitt, M., 2020. Using $^{87}Sr/^{86}Sr$ LA-MC-ICP-MS transects within modern and ancient calcite crystals to determine fluid flow events in deep granite fractures. Geosciences 10, 345.

Drake, H., Tullborg, E.-L., Page, L.M., 2009. Distinguished multiple events of fracture mineralisation related to far-field orogenic effects in Paleoproterozoic crystalline rocks, Simpevarp area, SE Sweden. Lithos 110, 37–49.

Ebert, K., Hättestrand, C., Hall, A.M., Alm, G., 2011. DEM identification of macro-scale stepped relief in arctic northern Sweden. Geomorphology 132, 339–350.

Eensaar, J., Gaškov, M., Pani, T., Sepp, H., Somelar, P., Kirsimäe, K., 2017. Hydrothermal fracture mineralization in the stable cratonic northern part of the Baltic Paleobasin: sphalerite fluid inclusion evidence. Geol. Foeren. Stockholm Foerh. 139, 52–62.

Elminen, T., Zwingmann, H., Kaakinen, A., 2018. Constraining the timing of brittle deformation and sedimentation in southern Finland: implications for Neoproterozoic evolution of the eastern Fennoscandian shield. Precambr. Res. 304, 110–124.

Elo, S., Kuivasaari, T., Lehtinen, M., Sarapää, O., Uutela, A., 1993. Iso-Naakkima, a circular structure filled with Neoproterozoic sediments, Pieksämäki, south-eastern Finland. Bull. Geol. Soc Finland 65, 3–30.

Eyles, N., de Broekert, P., 2001. Glacial tunnel valleys in the Eastern Goldfields of Western Australia cut below the Late Paleozoic Pilbara ice sheet. Palaeogeogr. Palaeoclimatol. Palaeoecol. 171, 29–40.

Fairbridge, R.W., Finkl, C.W., 1980. Cratonic erosional unconformities and peneplains. J. Geol. 88, 69–86.

Flowers, R.M., Bowring, S.A., Reiners, P.W., 2006. Low long-term erosion rates and extreme continental stability documented by ancient (U-Th)/He dates. Geology 34, 925–928.

Fontana, J., 2006. Phoscorite-carbonatite pipe complexes. Platin. Met. Rev. 50, 134–142.

Fox, M., Tripathy-Lang, A., Shuster, D., Winn, C., Karlstrom, K., Kelley, S., 2017. Westernmost Grand Canyon incision: testing thermochronometric resolution. Earth Planet. Sci. Lett. 474, 248–256.

Friese, N., Vollbrecht, A., Leiss, B., Jacke, O., 2011. Cambrian sedimentary dykes in the Proterozoic basement of the Västervik area (southeast Sweden): episodic formation inferred from macro-and microfabrics. Int. J. Earth Sci. 100, 741–752.

Gabrielsen, R.H., Nystuen, J.P., Jarsve, E.M., Lundmark, A.M., 2015. The Sub-Cambrian Peneplain in southern Norway: its geological significance and its implications for post-Caledonian faulting, uplift and denudation. J. Geol. Soc. 172, 777–791.

Gibbard, P., Lewin, J., 2016. Filling the North Sea Basin: Cenozoic sediment sources and river styles. Geol. Belgica 19, 201–217.

Gilg, H.A., Hall, A.M., Ebert, K., Fallick, A.E., 2013. Cool kaolins in Finland. Palaeogeogr. Palaeoclimatol. Palaeoecol. 392, 454–462.

Godard, A., 1965. Recherches de géomorphologie en Écosse du Nord-Ouest. Masson et Cie, Paris.

Gradstein, F.M., Ogg, J.G., Schmitz, M., Ogg, G., 2012. The Geologic Time Scale. Elsevier.

Grahn, Y., Nõlvak, J., Paris, F., 1996. Precise chitinozoan dating of Ordovician impact events in Baltoscandia. J. Micropalaeontol. 15, 21–35.

Green, P.F., Japsen, P., Bonow, J.M., Chalmers, J.A., Duddy, I.R., 2020. Thermal history solutions from thermochronology must be governed by geological relationships: a comment on Jess et al .(2019). Geomorphology 360, 106848.

Gudmundsson, A., 1983. Form and dimensions of dykes in eastern Iceland. Tectonophysics 95, 295–307.

Gunnell, Y., 2000. Apatite fission track thermochronology: an overview of its potential and limitations in geomorphology. Basin Res. 12, 115–132.

Gunnell, Y., 2020. Landscape evolution of Dartmoor, SW England: A review of evidence-based controversies and their wider implications for geoscience. Proceedings of the Geologists' Association 131, 187–226.

Gunnell, Y., Carter, A., Petit, C., Fournier, M., 2007. Post-rift seaward downwarping at passive margins: new insights from southern Oman using stratigraphy to constrain apatite fission-track and (U-Th)/He dating. Geology 35, 647–650.

Hagenfeldt, S.E., 1995. Erratics and Proterozoic-Lower Palaeozoic submarine sequences between Åland and mainland Sweden. Sveriges Geologiska Undersokning C84, pp. 1-33.

Haines, P., 2005. Impact cratering and distal ejecta: the Australian record. Aust. J. Earth Sci. 52, 481–507.

Hall, A.M., 1991. Pre-Quaternary landscape evolution in the Scottish Highlands. Trans. R. Soc. Edinburgh: Earth Sci. 82, 1–26.

Hall, A.M., 2015. Phanerozoic denudation across the Kola Peninsula, northwest Russia: implications for long term stability of Precambrian shield margins. Norw. J. Geol. 95, 27–43.

Hall, A.M., Ebert, K., Goodfellow, B.W., Hättestrand, C., Heyman, J., Krabbendam, M., Moon, S., Stroeven, A.P., 2019a. Past and future impact of glacial erosion in Forsmark and Uppland. Svensk Kärnbränslehantering AB. SKB TR-19-07 247.

Hall, A.M., Krabbendam, M., van Boeckel, M., Ebert, K., Hättestrand, C., Heyman, J., 2019b. The sub-Cambrian unconformity in Västergötland: Reference Surface for Glacial Erosion of Basement, Technical Report. Svensk Kärnbränslehantering AB. SKB TR-19-21 159.

Hall, A.M., Sarala, P., Ebert, K., 2015. Late Cenozoic deep weathering patterns on the Fennoscandian shield in northern Finland: a window on ice sheet bed conditions at the onset of Northern Hemisphere glaciation. Geomorphology 246, 472–488.

Hall, A.M., van Boeckel, M., 2020. Origin of the Baltic Sea basin by Pleistocene glacial erosion. Geol. Foeren. Stockholm Foerh. 142, 237–252.

Hanski, E., Huhma, H., Lahaye, Y., Lunkka, J.P., Nilsson, E., Mäki, T., O'Brien, H., Strand, K., 2019. Zn-Pb-Cu sulfide-bearing glacial sandstone erratics near Raahe on

the western coast of Finland: indicators of Paleozoic base metal mineralization at the bottom of the Bothnian Bay. Bull. Geol. Soc. Finland 91, 143–178.
Hawthorne, J., 1975. Model of a kimberlite pipe. Phys. Chem. Earth. 9, 1–15.
Hendriks, B., Andriessen, P., Huigen, Y., Leighton, C., Redfield, T., Murrell, G., Gallagher, K., Nielsen, S.B., 2007. A fission track data compilation for Fennoscandia. Norw. J. Geol. 87, 143–155.
Hendriks, B., Redfield, T., 2005. Apatite fission track and (U-Th)/He data from Fennoscandia: An example of underestimation of fission track annealing in apatite. Earth Planet. Sci. Lett. 236, 443–458.
Hendriks, B., Redfield, T., 2006. Reply to: Comment on "Apatite Fission Track and (U–Th)/He data from Fennoscandia: an example of underestimation of fission track annealing in apatite" by BWH Hendriks and TF Redfield. Earth Planet. Sci. Lett. 248, 569–577.
Hietala, S., Moilanen, J., 2007. Keurusselkä-Distribution of shatter cones, Lunar and Planetary Science Conference, p. 1762.
Hietala, S., Kreitsmann, T., Plado, J., Nenonen, J., Lerssi, J., Pesonen, L., 2020. Summanen Impact Structure—New Geological and Preliminary Geophysical Studies. LPI Contributions 2251, 2048.
Högbom, A.G., 1910. Precambrian geology of Sweden. Bull. Geol. Inst. Upsala 10, 1–80.
Holm, P.M., Pedersen, L.E., Højsteen, B., 2010. Geochemistry and petrology of mafic Proterozoic and Permian dykes on Bornholm, Denmark: four episodes of magmatism on the margin of the Baltic Shield. Bull. Geol. Soc. Den. 58, 35–65.
Holm, S., Alwmark, C., Alvarez, W., Schmitz, B., 2011. Shock barometry of the Siljan impact structure, Sweden. Meteorit. Planet. Sci. 46, 1888–1909.
Huhta, P., 1997. Almost 100 m of Quaternary deposits on sandstone at Karhukangas, Kauhajoki, western Finland, in: Autio, S. (Ed.), Geological Survey of Finland, Current Research 1995-1996, pp. 89–91.
Huigen, Y., Andriessen, P., 2004. Thermal effects of Caledonian foreland basin formation, based on fission track analyses applied on basement rocks in central Sweden. Phys. Chem. Earth, Parts A/B/C 29, 683–694.
Isozaki, Y., Põldvere, A., Bauert, H., Nakahata, H., Aoki, K., Sakata, S., Hirata, T., 2014. Provenance shift in Cambrian mid-Baltica: detrital zircon chronology of Ediacaran-Cambrian sandstones in Estonia. Estonian J. Earth Sci. 63.
Ivleva, A.S., Podkovyrov, V.N., Ershova, V.B., Khubanov, V.B., Khudoley, A.K., Sychev, S. N., Vdovina, N.I., Maslov, A.V., 2018. U-Pb LA–ICP–MS age of detrital zircons from the lower Riphean and upper Vendian deposits of the Luga-Ladoga Monocline. Dokl. Earth Sci. 480, 695–699.
Japsen, P., Green, P.F., Bonow, J.M., Erlström, M., 2016. Episodic burial and exhumation of the southern Baltic Shield: Epeirogenic uplifts during and after break-up of Pangaea. Gondwana Res. 35, 357–377.
Järvelä, J., Pesonen, L., Pietarinen, H., 1995. On palaeomagnetism and petrophysics of the Iso-Naakkima impact structure, southeastern Finland. GTK Open File Report Q19.
Jõeleht, A., Plado, J., Sarv, K., 2018. Kärdla impact crater–transitional from simple to complex based on reflection seismics. EPSC Abstracts 12.
Jourdan, F., Reimold, W.U., Deutsch, A., 2012. Dating terrestrial impact structures. Elements 8, 49–53.
Jourdan, F., Renne, P., Reimold, W., 2008. High-precision $^{40}Ar/^{39}Ar$ age of the Jänisjärvi impact structure (Russia). Earth Planet. Sci. Lett. 265, 438–449.
Juhlin, C., Sturkell, E., Ebbestad, J.O.R., Lehnert, O., Högström, A.E., Meinhold, G., 2012. A new interpretation of the sedimentary cover in the western Siljan Ring area, central Sweden, based on seismic data. Tectonophysics 580, 88–99.
Karhu, J., 2000. Carbon, oxygen and strontium isotopic characteristics of late-stage fracture calcites at Olkiluoto and Romuvaara, Working Report 2000-19, Geological Survey of Sweden.
Kenny, G.G., Mänttäri, I., Schmieder, M., Whitehouse, M.J., Nemchin, A.A., Bellucci, J.J., Merle, R.E., 2020. The age of the Sääksjärvi impact structure (Finland): reconciling the timing of small impacts in crystalline basement with that of regional basin development. J. Geol. Soc. 177, 1231–1243.
Kenny, G.G., Schmieder, M., Whitehouse, M.J., Nemchin, A.A, Morales, L.F, Buchner, E., Bellucci, J.J., Snape, J.F., 2019. A new U-Pb age for shock-recrystallised zircon from the Lappajärvi impact crater, Finland, and implications for the accurate dating of impact events. Geochim. Cosmochim. Acta 245, 479–494.
Kietäväinen, R., Ahonen, L., Kukkonen, I.T., Niedermann, S., Wiersberg, T., 2014. Noble gas residence times of saline waters within crystalline bedrock, Outokumpu Deep Drill Hole, Finland. Geochim. Cosmochim. Acta 145, 159–174.
Kirsimäe, K., Jørgensen, P., Kalm, V., 1999. Low-temperature diagenetic illite-smectite in Lower Cambrian clays in North Estonia. Clay Miner. 34, 151–163.
Kirsimäe, K., Melezhik, V.A., 2013. Palaeoproterozoic Weathered Surfaces. In: Kump, L. R., Kirsimäe, K., Melezhik, V.A., Brasier, A.T., Fallick, A.E., Salminen, P.E. (Eds.), Reading the Archive of Earth's Oxygenation. Springer, pp. 1409–1417.
Kohn, B., Gleadow, A., 2019. Application of low-temperature thermochronology to craton evolution. In: Malusà, M.G., Fitzgerald, P.G. (Eds.), Fission-Track Thermochronology and its Application to Geology. Springer International Publishing, Cham, pp. 373–393.
Kohn, B.P., Lorencak, M., Gleadow, A.J.W., Kohlmann, F., Raza, A., Osadetz, K.G., Sorjonen-Ward, P., 2009. A reappraisal of low-temperature thermochronology of the eastern Fennoscandia Shield and radiation-enhanced apatite fission-track annealing. Geol. Soc., London, Spec. Publ. 324, 193–216.
Kohonen, J., Rämö, O.T., 2005. Sedimentary rocks, diabases, and late cratonic evolution. In: Lehtinen, M.J., Numri, A.P., Rämö, O.T. (Eds.), Precambrian Geology of Finland - Key to the Evolution of the Fennoscandian Shield. Elsevier, Amsterdam, pp. 563–603.
Koistinen, T., Stephens, M., Bogatchev, V., Nordgulen, Ø., Wennerström, M., Korhonen, J., 2001. Geological map of the Fennoscandian Shield 1: 2 000 000, Espoo, Trondheim, Uppsala, Moscow. Geol surveys of Finland, Norway, Sweden, Ministry of Natural Resources, Russia.
Koistinen, T.J., 1996. Explanation to the Map of Precambrian basement of the Gulf of Finland and surrounding area 1:1 million. Geological Survey of Finland, Espoo.
Korja, A., Lahtinen, R., Nironen, M., 2006. The Svecofennian orogen: a collage of microcontinents and island arcs. Geol. Soc., London, Memoirs 32, 561–578.
Kukkonen, I.T., Lahtinen, R., 2001. Variation of radiogenic heat production rate in 2.8–1.8 Ga old rocks in the central Fennoscandian shield. Phys. Earth Planet. Inter. 126, 279–294.
Kuznetsov, N., Orlov, S.Y., Miller, E., Shazillo, A., Dronov, A., Soboleva, A., Udoratina, O., Gehrels, G., 2011. First results of U/Pb dating of detrital zircons from early Paleozoic and Devonian sandstones of the Baltic-Ladoga region (south Ladoga area). In: Doklady Earth Sciences. Springer, pp. 759–765.
Lahtinen, R., Nironen, M., 2010. Paleoproterozoic lateritic paleosol–ultra-mature/mature quartzite–meta-arkose successions in southern Fennoscandia—intra-orogenic stage during the Svecofennian orogeny. Precambr. Res. 183, 770–790.
Laitakari, I., Leino, H., 1989. A new model for the emplacement of the Häme diabase dyke swarm, central Finland, Geological Survey of Finland Current Research 1988. Geological Survey of Finland Espoo, pp. 7-8.
Larson, S.-A., Tullborg, E.-L., Cederbom, C., Stiberg, J.-P., 1999. Sveconorwegian and Caledonian foreland basins in the Baltic Shield revealed by fission-track thermochronology. Terra Nova-Oxford 11, 210–215.
Larson, S.Å., Cederbom, C.E., Tullborg, E.-L., Stiberg, J.-P., 2006. Comment on "Apatite fission track and (U–Th)/He data from Fennoscandia: an example of underestimation of fission track annealing in apatite" by Hendriks and Redfield [Earth Planet. Sci. Lett. 236 (443–458)]. Earth Planet. Sci. Lett. 248, 561–568.
Lehtovaara, J.J., 1982. Stratigraphical section through Lower Cambrian at Söderfjärden, Vaasa, western Finland. Bull. Geol. Soc. Finland 54, 35–43.
Lidmar-Bergström, K., 1988. Denudation surfaces of a shield area in south Sweden. Geografiska Annaler. Series A. Physical Geography, pp. 337-350.
Lidmar-Bergström, K., 1993. Denudation surfaces and tectonics in the southernmost part of the Baltic Shield. Precambr. Res. 64, 337–345.
Lidmar-Bergström, K., 1995. Relief and saprolites through time on the Baltic Shield. Geomorphology 12, 45–61.
Lidmar-Bergström, K., Olsson, S., Olvmo, M., 1997. Palaeosurfaces and associated saprolites in southern Sweden. In: Widdowson, M. (Ed.), Palaeosurfaces: Recognition, Reconstruction and Palaeoenvironmental Interpretation. The Geological Society, London, pp. 95–124.
Lidmar-Bergström, K., Olvmo, M., 2015. Plains, steps, hilly relief and valleys in northern Sweden – review, interpretations and implications for conclusions on Phanerozoic tectonics. SGU Research Paper C 838, pp. 1-42.
Liivamägi, S., Somelar, P., Mahaney, W.C., Kirs, J., Vircava, I., Kirsimäe, K., 2014. Late Neoproterozoic Baltic paleosol: intense weathering at high latitude? Geology 42, 323–326.
Lindqvist, K., Laitakari, I., 1980. Glass and amygdules in Precambrian diabases from Orivesi, southern Finland. Bullet. Geol. Soc. Finland 52, 221–229.
Lindström, M., Sturkell, E.F.F., Törnberg, R., Ormouml, J., 1996. The marine impact crater at Lockne, central Sweden. GFF 118, 193–206.
Lundmark, A.M., Lamminen, J., 2016. The provenance and setting of the Mesoproterozoic Dala Sandstone, western Sweden, and paleogeographic implications for southwestern Fennoscandia. Precambr. Res. 275, 197–208.
Łuszczak, K., Persano, C., Braun, J., Stuart, F.M., 2017. How local crustal thermal properties influence the amount of denudation derived from low-temperature thermochronometry. Geology 45, 779–782.
Mark, D.F., Lindgren, P., Fallick, A.E., 2014. A high-precision $^{40}Ar/^{39}Ar$ age for hydrated impact glass from the Dellen impact, Sweden. Geol. Soc., London, Spec. Publ. 378, 349–366.
Masaitis, V., 1999. Impact structures of northeastern Eurasia: The territories of Russia and adjacent countries. Meteorit. Planet. Sci. 34, 691–711.
Masaitis, V., 2005. Morphological, structural and lithological records of terrestrial impacts: an overview. Aust. J. Earth Sci. 52, 509–528.
McDannell, K.T., Issler, D.R., O'Sullivan, P.B., 2019. Radiation-enhanced fission track annealing revisited and consequences for apatite thermochronometry. Geochim. Cosmochim. Acta 252, 213–239.
Meert, J.G., Walderhaug, H.J., Torsvik, T.H., Hendriks, B.W.H., 2007. Age and paleomagnetic signature of the Alnø carbonatite complex (NE Sweden): Additional controversy for the Neoproterozoic paleoposition of Baltica. Precambr. Res. 154, 159–174.
Mertanen, S., 2008. Paleomagnetism of diabase dykes, pegmatitic granites and TGG gneisses in the Olkiluoto area. 2007-96 Posiva Oy.
Merrill, G.K., 1980. Ordovician conodonts from the Åland Islands, Finland. Geologiska Föreningen i Stockholm Förhandlingar 101, 329–341.
Mertanen, S., Airo, M.-L., Elminen, T., Niemelä, R., Pajunen, M., Wasenius, P., Wennerström, M., 2008. Paleomagnetic evidence for Mesoproterozoic-Paleozoic reactivation of the Paleoproterozoic crust in southern Finland. Geol. Surv. Finland Spec. Pap. 47, 215–252.
Miller, E.L., Kuznetsov, N., Soboleva, A., Udoratina, O., Grove, M., Gehrels, G., 2011. Baltica in the Cordillera? Geology 39, 791–794.
Mordberg, L.E., Nesterova, E.N., 1996. Palaeozoic bauxite deposits of North Onega basin, Russia: evidence as to genesis. Transactions of the Institution of Mining and Metallurgy. Sect. B. Appl. Earth Sci. 105, 200–205.
Murrell, G.R., Andriessen, P.A.M., 2004. Unravelling a long-term multi-event thermal record in the cratonic interior of southern Finland through apatite fission track thermochronology. Phys. Chem. Earth, Parts A/B/C 29, 695–706.
Mutanen, T., 1979. Sääksjärvi on sittenkin astrobleemi. Geologi 31, 125–130.

Nielsen, A.T., Schovsbo, N.H., 2011. The Lower Cambrian of Scandinavia: depositional environment, sequence stratigraphy and palaeogeography. Earth Sci. Rev. 107, 207–310.
Nielsen, A.T., Schovsbo, N.H., 2015. The regressive Early-Mid Cambrian 'Hawke Bay Event'in Baltoscandia: epeirogenic uplift in concert with eustasy. Earth Sci. Rev. 151, 288–350.
Nironen, M., 2017. Guide to the Geological Map of Finland–Bedrock 1: 1 000 000. Geological Survey of Finland, Special Paper 60, pp. 41-76.
O'Brien, H.E., Tynni, M., 1998. Mineralogy and geochemistry of kimberlites and related rocks from Finland, In: International Kimberlite Conference: Extended Abstracts, pp. 643-645.
O'Brien, H.E., 2015. Kimberlite-hosted diamonds in Finland. In: Maier, W.D., Lahtinen, R., O'Brien, H.E. (Eds.), Mineral Deposits of Finland. Elsevier, pp. 345–375.
Öhman, T., 2002. The indications of cratering process in Saarijärvi impact crater, northern Finland. University of Oulu, Finland.
Öhman, T., 2007. The origin and tectonic modification of the Saarijärvi impact structure, northern Finland. Workshop on Impact Cratering II. Lunar and Planetary Institute, Houston, Texas: Saint-Hubert, Canada 85–86.
Öhman, T., Preeden, U., 2013. Shock metamorphic features in quartz grains from the Saarijärvi and Söderfjärden impact structures, Finland. Meteorit. Planet. Sci. 48, 955–975.
Ormö, J., 1994. The pre-impact Ordovician stratigraphy of the Tvären Bay impact structure, SE Sweden. GFF 116, 139–144.
Örmö, J., Sturkell, E., Nölvak, J., Melero-Asensio, I., Frisk, Å., Wikström, T., 2014. The geology of the Målingen structure: A probable doublet to the Lockne marine-target impact crater, central Sweden. Meteorit. Planet. Sci. 49, 313–327.
Osinski, G.R., Ferrière, L., 2016. Shatter cones:(Mis) understood? Sci. Adv. 2, e1600616.
Osinski, G.R., Grieve, R.A., Bleacher, J.E., Neish, C.D., Pilles, E.A., Tornabene, L.L., 2018. Igneous rocks formed by hypervelocity impact. J. Volcanol. Geoth. Res. 353, 25–54.
Page, L., Hermansson, T., Söderlund, P., Stephens, M., 2007. Forsmark Site Investigation: $^{40}Ar/^{39}Ar$ and (U-Th)/He Geochronology. Svensk Kärnbränslehantering AB. SKB P-06-211.
Parnell, J., Mark, D.F., Frei, R., Fallick, A.E., Ellam, R.M., 2014. $^{40}Ar/^{39}Ar$ dating of exceptional concentration of metals by weathering of Precambrian rocks at the Precambrian-Cambrian boundary. Precambr. Res. 246, 54–63.
Paulamäki, S., Kuivamäki, A., 2006. Depositional history and tectonic regimes within and in the margins of the Fennoscandian Shield during the last 1300 million years, Working Report. Geological Survey of Finland, pp. 1-137.
Perttunen, V., 1970. Lokkaite, a new hydrous RE-carbonate from Pyörönmaa pegmatite in Kangasala, SW Finland. Bull. Geol. Soc. Finland 43, 67–72.
Pesonen, L.J., Elo, S., Lehtinen, M., Jokinen, T., Puranen, R., Kivekas, L., 1999. Lake Karikkoselkä impact structure, central Finland; new geophysical and petrographic results. In: Special Paper - Geological Society of America, pp. 131–147.
Pesonen, L.J., Järvelä, J., Sarapää, O., Pietarinen, H., 1996. The Iso-Naakkima meteorite impact structure: physical properties and paleomagnetism of a drill core. Meteorit. Planet. Sci. Suppl. 31, 105–106.
Peters, S.E., Gaines, R.R., 2012. Formation of the 'Great Unconformity' as a trigger for the Cambrian explosion. Nature 484, 363–366.
Peulvast, J.-P., Bétard, F., Lageat, Y., 2009. Long-term landscape evolution and denudation rates in shield and platform areas: a morphostratigraphic approach. Géomorphologie 2, 95–108.
Peulvast, J.-P., Bouchard, M., Jolicoeur, S., Pierre, G., Schroeder, J., 1996. Palaeolandforms and morphotectonic evolution around the Baie des Chaleurs (eastern Canada). Geomorphology 16, 5–32.
Peulvast, J.-P., Claudino Sales, V., Bétard, F., Gunnell, Y., 2008. Low post-Cenomanian denudation depths across the Brazilian Northeast: Implications for long-term landscape evolution at a transform continental margin. Global Planet. Change 62, 39–60.
Pitkäranta, R., 2013. Lithostratigraphy and age of pre-Late Weichselian sediments in the Suupohja area, western Finland. Turku, p. 66.
Plado, J., 2012. Meteorite impact craters and possibly impact-related structures in Estonia. Meteorit. Planet. Sci. 47, 1590–1605.
Plado, J., Hietala, S., Kreitsmann, T., Lerssi, J., Nenonen, J., Pesonen, L.J., 2018. Summanen, a new meteorite impact structure in Central Finland. Meteorit. Planet. Sci. 53, 2413–2426.
Pokki, J., Kohonen, J., Lahtinen, R., Rämö, O., Andersen, T., 2013a. Petrology and provenance of the Mesoproterozoic Satakunta sandstone, SW Finland. Geological Survey of Finland, Report of Investigation 204, 47.
Pokki, J., Kohonen, J., Rämö, O.T., Andersen, T., 2013b. The Suursaari conglomerate (SE Fennoscandian shield; Russia)—Indication of cratonic conditions and rapid reworking of quartz arenitic cover at the outset of the emplacement of the rapakivi granites at ca. 1.65Ga. Precambr. Res. 233, 132–143.
Poprawa, P., Šliaupa, S., Stephenson, R., Lazauskiene, J., 1999. Late Vendian-Early Palæozoic tectonic evolution of the Baltic Basin: regional tectonic implications from subsidence analysis. Tectonophysics 314, 219–239.
Preeden, U., Mertanen, S., Elminen, T., Plado, J., 2009. Secondary magnetizations in shear and fault zones in southern Finland. Tectonophysics 479, 203–213.
Pulsipher, M.A., Dehler, C.M., 2019. U-Pb detrital zircon geochronology, petrography, and synthesis of the middle Neoproterozoic Visingsö Group, Southern Sweden. Precambr. Res. 320, 323–333.
Punkari, M., 1994. Function of the ice streams in the Scandinavian ice sheet: analyses of glacial geological data from southwestern Finland. Trans. R. Soc. Edinburgh: Earth Sci. 85, 283–302.
Puura, V., Amantov, A., Tikhomirov, S., Laitakari, I., 1996. Latest events affecting the Precambrian basement, Gulf of Finland and surrounding areas, in: Koistinen, T. (Ed.), Explanation to the Map of Precambrian Basement of the Gulf of Finland and Surrounding Areas. Geological Survey of Finland, Espoo, pp. 115–125.
Puura, V., Flodén, T., 1999. Rapakivi-granite–anorthosite magmatism — a way of thinning and stabilisation of the Svecofennian crust, Baltic Sea Basin. Tectonophysics 305, 75–92.
Puura, V., Plado, J., 2005. Settings of meteorite impact structures in the Svecofennian crustal domain. In: Koeberl, C., Henkel, H. (Eds.), Impact Tectonics. Springer, pp. 211–245.
Raiskila, S., Plado, J., Ruotsalainen, H., Pesonen, L., 2013. Geophysical signatures of the Keurusselkä meteorite impact structure-implications for crater dimensions. Geophysica 49, 3–23.
Raiskila, S., Salminen, J., Elbra, T., Pesonen, L.J., 2011. Rock magnetic and paleomagnetic study of the Keurusselkä impact structure, central Finland. Meteorit. Planet. Sci. 46, 1670–1687.
Rajala, P., Bomberg, M., Kietäväinen, R., Kukkonen, I., Ahonen, L., Nyyssönen, M., Itävaara, M., 2015. Rapid Reactivation of deep subsurface microbes in the presence of C-1 compounds. Microorganisms 3, 17–33.
Rasmussen, E.S., 2018. Discussion of "Eocene to mid-Pliocene landscape evolution in Scandinavia inferred from offshore sediment volumes and pre-glacial topography using inverse modelling"(Pedersen et al. 2018. Geomorphology, 303: 467–485). Geomorphology 328, 222–224.
Reddy, M., Glorie, S., Reid, A.J., Collins, A.S., 2015. Phanerozoic cooling history of the central Gawler Craton: implications of new low-temperature thermochronological data. Mesa J. 75, 56–60.
Rice-Bredin, S., 2012. Paragenesis and fluid history of the Karku unconformity-uranium deposit, Pasha-Ladoga Basin. Western Russia. Queen's University, Kingston, Ontario, Canada.
Ripa, M., Stephens, M.B., 2020. Chapter 13 Siliciclastic sedimentation in a foreland basin to the Sveconorwegian orogen and dolerites (0.98–0.95 Ga) related to intracratonic rifting. Geol. Soc., London, Memoirs 50, 325–333.
Rudberg, S., 1970. The sub-Cambrian peneplain in Sweden and its slope gradient. Z. Geomorph. NF 9, 157–167.
Sahlstedt, E., Karhu, J., Pitkänen, P., Whitehouse, M., 2013. Implications of sulfur isotope fractionation in fracture-filling sulfides in crystalline bedrock, Olkiluoto, Finland. Appl. Geochem. 32, 52–69.
Saintot, A., Stephens, M., Viola, G., Nordgulen, Ø., 2011. Brittle tectonic evolution and paleostress field reconstruction in the southwestern part of the Fennoscandian Shield. Forsmark, Sweden. Tectonics 30, 1–36.
Salminen, J., Klein, R., Veikkolainen, T., Mertanen, S., Mänttäri, I., 2017. Mesoproterozoic geomagnetic reversal asymmetry in light of new paleomagnetic and geochronological data for the Häme dyke swarm, Finland: implications for the Nuna supercontinent. Precambr. Res. 288, 1–22.
Samuelsson, J., Middleton, M.F., 1998. The Caledonian foreland basin in Scandinavia: constrained by the thermal maturation of the Alum Shale. Geol. Foeren. Stockholm Foerh. 120, 307–314.
Sandström, B., Tullborg, E.-L., 2009. Episodic fluid migration in the Fennoscandian Shield recorded by stable isotopes, rare earth elements and fluid inclusions in fracture minerals at Forsmark, Sweden. Chem. Geol. 266, 126–142.
Sandström, B., Tullborg, E.-L., Torres, T.D., Ortiz, J.E., 2006. The occurrence and potential origin of asphaltite in bedrock fractures, Forsmark, central Sweden. Geol. Foeren. Stockholm Foerh. 128, 233–242.
Sarapää, O., 1996. Proterozoic primary kaolin deposits at Virtasalmi, southeastern Finland. Geol. Surv. Finland Spec. Publ. 18b, 1–152.
Schmieder, M., Jourdan, F., 2013. The Lappajärvi impact structure (Finland): age, duration of crater cooling, and implications for early life. Geochim. Cosmochim. Acta 112, 321–339.
Schmieder, M., Jourdan, F., Hietala, S., Moilanen, J., Öhman, T., Buchner, E., 2009. A High-Precision late Mesoproterozoic $^{40}Ar/^{39}Ar$ age for the Keurusselkä impact structure (Finland). Proceedings of Lunar and Planetary Science Conference 40, 1028.
Schmieder, M., Jourdan, F., Moilanen, J., Buchner, E., Öhman, T., 2016a. A Late Mesoproterozoic $^{40}Ar/^{39}Ar$ age for a melt breccia from the Keurusselkä impact structure, Finland. Meteorit. Planet. Sci. 51, 303–322.
Schmieder, M., Jourdan, F., Öhman, T., Tohver, E., Mayers, C., Frew, A., 2014. A Proterozoic $^{40}Ar/^{39}Ar$ age for the Söderfjärden impact structure, Finland. In: Lunar and Planetary Science Conference, pp. 1301.
Schmieder, M., Kring, D.A., 2020. Earth's Impact events through geologic time: a list of recommended ages for terrestrial impact structures and deposits. Astrobiology 20, 91–141.
Schmieder, M., Moilanen, J., Buchner, E., 2008. Impact melt rocks from the Paasselkä impact structure (SE Finland): petrography and geochemistry. Meteorit. Planet. Sci. 43, 1189–1200.
Schmieder, M., Schwarz, W.H., Buchner, E., Trieloff, M., Moilanen, J., Öhman, T., 2010. A Middle-Late Triassic $^{40}Ar/^{39}Ar$ age for the Paasselkä impact structure (SE Finland). Meteorit. Planet. Sci. 45, 572–582.
Schmieder, M., Schwarz, W.H., Trieloff, M., Buchner, E., Hopp, J., Tohver, E., Pesonen, L. J., Lehtinen, M., Moilanen, J., Werner, S.C., Öhman, T., 2016b. The two Suvasvesi impact structures, Finland: Argon isotopic evidence for a "false" impact crater doublet. Meteorit. Planet. Sci. 51, 966–980.
Schmieder, M., Schwarz, W.H., Trieloff, M., Tohver, E., Buchner, E., Hopp, J., Osinski, G. R., 2015. New $^{40}Ar/^{39}Ar$ dating of the Clearwater Lake impact structures (Québec, Canada)–not the binary asteroid impact it seems? Geochim. Cosmochim. Acta 148, 304–324.
Schwarz, W.H., Schmieder, M., Buchner, E., Trieloff, M., Moilanen, J., Öhman, T., 2015. A Carnian $^{40}Ar/^{39}Ar$ age for the Paasselkä impact structure (SE Finland)—an update. Meteorit. Planet. Sci. 50, 135–140.

Simonen, A., 1960. Pre-quaternary rocks in Finland. Bull. Commission Géologique Finlande 191, 1–49.
Slagstad, T., Marker, M., Roberts, N.M.W., Saalmann, K., Kirkland, C.L., Kulakov, E., Ganerød, M., Røhr, T.S., Møkkelgjerd, S.H.H., Granseth, A., Sørensen, B.E., 2020. The Sveconorwegian orogeny – reamalgamation of the fragmented southwestern margin of Fennoscandia. Precambr. Res. 350, 105877.
Slater, B.J., Willman, S., 2019. Early Cambrian small carbonaceous fossils (SCFs) from an impact crater in western Finland. Lethaia 52, 570–582.
Šliaupa, S., Hoth, P., 2011. Geological evolution and resources of the Baltic Sea area from the Precambrian to the Quaternary. In: Harff, J., Björck, S., Hoth, P. (Eds.), The Baltic Sea Basin. Springer, Berlin Heidelberg, pp. 13–51.
Söderberg, P., Hagenfeldt, S.E., 1995. Upper Proterozoic and Ordovician submarine outliers in the archipelago northeast of Stockholm, Sweden. Geol. Foeren. Stockholm Foerh. 117, 153–161.
Söderman, G., 1985. Planation and weathering in eastern Fennoscandia. Fennia 163, 347–352.
Söderman, G., Kejonen, A., Kujansuu, R., 1983. The riddle of the tors at Lauhavuori, western Finland. Fennia 161, 91–144.
Soomer, S., Somelar, P., Mänd, K., Driese, S.G., Lepland, A., Kirsimäe, K., 2019. High-CO_2, acidic and oxygen-starved weathering at the Fennoscandian Shield at the Archean-Proterozoic transition. Precambr. Res. 327, 68–80.
Stanley, J.R., Flowers, R.M., Bell, D.R., 2013. Kimberlite (U-Th)/He dating links surface erosion with lithospheric heating, thinning, and metasomatism in the southern African Plateau. Geology 41, 1243–1246.
Stewart, A.D., 1972. Precambrian landscapes in northwest Scotland. Geol. J. 8, 111–124.
Strand, K., 2012. Sequence stratigraphy of the Karelian formations (2.4–2.0 Ga) of the Fennoscandian Shield – significance of major unconformities. Mar. Pet. Geol. 33, 117–126.
Stuevold, L.M., Eldholm, O., 1996. Cenozoic uplift of Fennoscandia inferred from a study of the mid-Norwegian margin. Global Planet. Change 12, 359–386.
Sturkell, E., Lindström, M., 2004. The target peneplain of the Lockne impact. Meteorit. Planet. Sci. 39, 1721–1731.
Sturt, B.A., Melezhik, V.A., Ramsay, D.M., 1994. Early Proterozoic regolith at Pasvik, NE Norway: palaeoenvironmental implications for the Baltic Shield. Terra Nova 6, 618–633.
Suuroja, S., Suuroja, K., 2004. The Neugrund marine impact structure (Gulf of Finland, Estonia). In: Dypvik, H., Burchell, M.J., Claeys, P. (Eds.), Cratering in Marine Environments and on Ice. Springer, pp. 75–95.
Suuroja, K., Suuroja, S., 2010. The Neugrund meteorite crater on the seafloor of the Gulf of Finland, Estonia. Baltica 23, 47–58.
Suuroja, K., Suuroja, S., All, T., Floden, T., 2002. Kärdla (Hiiumaa Island, Estonia)—the buried and well-preserved Ordovician marine impact structure. Deep Sea Res. Part II 49, 1121–1144.
Talyzina, N.M., 1998. Fluorescence intensity in Early Cambrian acritarchs from Estonia. Rev. Palaeobot. Palynol. 100, 99–108.
Tanner, V., 1938. Die Oberflächengestaltung Finlands. Finska Vetenskaps. Soc.
Terekhov, E.N., Baluev, A.S., Kolodyazhnyi, S.Y., Belokrys, M.A., 2017. Trace elements in Upper Devonian rocks of the Andoma Hill zone of fold-and-fault dislocations (southeastern Onega region) as indicators of source areas. Lithol. Min. Resour. 52, 319–333.
Tikkanen, M., 2002. The changing landforms of Finland. Fennia 180, 21–30.
Torsvik, T.H., Cocks, L.R.M., 2016. Earth History and Palaeogeography. Cambridge University Press.
Tuisku, P., 2010. Heavy minerals from gold sluicings in lapland gold rush areas, and their bearing on the origin of gold bearing tills. In: Tuisku, P., Nemliher, J. (Eds.), Proceedings of the 5th Annual Meeting of Nordic Mineralogical Network. University of Oulu, Tallinn.
Tullborg, E.-L., Larson, S.A., Björklund, L., Samuelsson, L., Stigh, J., 1995. Thermal evidence of Caledonide foreland, molasse sedimentation in Fennoscandia. Svensk Kärnbränslehantering AB. SKB-TR–95-18.
Turtle, E., Pierazzo, E., Collins, G., Osinski, G., Melosh, H., Morgan, J., Reimold, W., 2005. Impact structures: What does crater diameter mean? Geol. Soc. Am. Spec. Pap. 384, 1–24.
Twidale, C.R., 2000. Early Mesozoic (? Triassic) landscapes in Australia: evidence, argument, and implications. J. Geol. 108, 537–552.
Twidale, C.R., Campbell, E.M., Bourne, A.J., 2020. Evolution of an ancient cratonic upland, the Gawler Ranges of inland South Australia. Géomorphol.: Relief, Processus, Environ. 26, 35–54.
Tynni, R., 1982. On Paleozoic microfossils in clastic dykes on the Åland Islands and in the core samples of Lumparn. Geol. Surv. Finland Bull. 317, 34–132.
Uutela, A., 1990. Proterozoic microfossils from the sedimentary rocks of Lappajärvi impact crater. Bull. Geol. Soc. Finland 62, 115–121.
Uutela, A., 2001. Proterozoic and early Palaeozoic microfossils in the Karikkoselkä impact crater, central Finland. Bullet. Geol. Soc. Finland 73, 75–85.
Vartiainen, H., 1980. The petrography, mineralogy and petrochemistry of the Sokli carbonatite massif, northern Finland. Geol. Survey Finland Bull. 313, 1–126.
Vasconcelos, P.M., Carmo, I.D.O., 2018. Calibrating denudation chronology through $^{40}Ar/^{39}Ar$ weathering geochronology. Earth Sci. Rev. 179, 411–435.
Veikkolainen, T., Kukkonen, I.T., 2019. Highly varying radiogenic heat production in Finland, Fennoscandian Shield. Tectonophysics 750, 93–116.
Velichkin, V., Tarasov, N., Andreeva, O., Kiseleva, G., Krylova, T., Doinikova, O., Golubev, V., Golovin, V., Kushnerenko, V., 2005. Geology and formation conditions of the Karku unconformity-type deposit in the northern Ladoga region (Russia). Geol. Ore Deposits 47, 87–112.
Veselovskiy, R.V., Thomson, S.N., Arzamastsev, A.A., Botsyun, S., Travin, A.V., Yudin, D. S., Samsonov, A.V., Stepanova, A.V., 2019. Thermochronology and exhumation history of the Northeastern Fennoscandian Shield Since 1.9 Ga: evidence From $^{40}Ar/^{39}Ar$ and Apatite Fission Track Data From the Kola Peninsula. Tectonics 38, 2317–2337.
von Eckermann, H., 1937. The Jotnian Formation and the sub-Jotnian unconformity. Geologiska Föreningen i Stockholm Förhandlingar 59, 19–58.
Vorma, A.I., 1975. On two roof pendants in the Wiborg rapakivi massif, southeastern Finland. Geol. Surv. Finland, Bull. 272, 1–86.
Webb, J.A., 2017. Denudation history of the Southeastern highlands of Australia. Aust. J. Earth Sci. 64, 841–850.
Werner, S.C., Plado, J., Pesonen, L.J., Janle, P., Elo, S., 2002. Potential fields and subsurface models of Suvasvesi North impact structure, Finland. Phys. Chem. Earth, Parts A/B/C 27, 1237–1245.
Wickström, L.M., Stephens, M.B., 2020. Chapter 18 Tonian–Cryogenian rifting and Cambrian–early Devonian platformal to foreland basin development outside the Caledonide orogen. Geol. Soc., London, Memoirs 50, 451–477.
Winterhalter, B., 1972. On the geology of the Bothnian Sea, an epeiric sea that has undergone Pleistocene glaciation. Geol. Surv. Finland Bull. 258, 1–74.
Winterhalter, B., Flodén, T., Ignatius, H., Axberg, S., Niemistö, L., 1981. Geology of the Baltic Sea. Elsevier Oceanogr. Ser. 30, 1–121.
Zapata, S., Sobel, E.R., del Papa, C., Jelinek, A., Glodny, J., 2019. Using a Paleosurface to Constrain Low-Temperature Thermochronological data: Tectonic Evolution of the Cuevas Range, Central Andes. Tectonics 38, 3939–3958.